



Paleoceanography

RESEARCH ARTICLE

10.1002/2015PA002837

Key Points:

- Seamount assemblages dominated by shallow infaunal suspension feeders
- Post-PETM faunas affected by ocean acidification and changes in current regime
- PETM and ETM3 associated with increased food supply through trophic focusing

Supporting Information:

- Figures S1–S8 and Captions for Tables S1–S5
- Table S1
- Table S2
- Table S3
- Table S4
- Table S5

Correspondence to:

G. J. Arreguín-Rodríguez,
arreguin@unizar.es

Citation:

Arreguín-Rodríguez, G. J., L. Alegret, and E. Thomas (2016), Late Paleocene-middle Eocene benthic foraminifera on a Pacific seamount (Allison Guyot, ODP Site 865): Greenhouse climate and superimposed hyperthermal events, *Paleoceanography*, 31, 346–364, doi:10.1002/2015PA002837.

Received 2 JUN 2015

Accepted 21 JAN 2016

Accepted article online 28 JAN 2016

Published online 1 MAR 2016

Late Paleocene-middle Eocene benthic foraminifera on a Pacific seamount (Allison Guyot, ODP Site 865): Greenhouse climate and superimposed hyperthermal events

Gabriela J. Arreguín-Rodríguez¹, Laia Alegret^{1,2}, and Ellen Thomas^{3,4}

¹Departamento de Ciencias de la Tierra, Universidad de Zaragoza, Zaragoza, Spain, ²Instituto Universitario de Ciencias Ambientales, Universidad de Zaragoza, Zaragoza, Spain, ³Department of Geology and Geophysics, Yale University, New Haven, Connecticut, USA, ⁴Department of Earth and Environmental Sciences, Wesleyan University, Middletown, Connecticut, USA

Abstract We investigated the response of late Paleocene-middle Eocene (~60–37.5 Ma) benthic foraminiferal assemblages to long-term climate change and hyperthermal events including the Paleocene-Eocene Thermal Maximum (PETM) at Ocean Drilling Program (ODP) Site 865 on Allison Guyot, a seamount in the Mid-Pacific Mountains. Seamounts are isolated deep-sea environments where enhanced current systems interrupt benthic-pelagic coupling, and fossil assemblages from such settings have been little evaluated. Assemblages at Site 865 are diverse and dominated by cylindrical calcareous taxa with complex apertures, an extinct group which probably lived infaunally. Dominance of an infaunal morphogroup is unexpected in a highly oligotrophic setting, but these forms may have been shallow infaunal suspension feeders, which were ecologically successful on the current-swept seamount. The magnitude of the PETM extinction at Site 865 was similar to other sites globally, but lower diversity postextinction faunas at this location were affected by ocean acidification as well as changes in current regime, which might have led to increased nutrient supply through trophic focusing. A minor hyperthermal saw less severe effects of changes in current regime, with no evidence for carbonate dissolution. Although the relative abundance of infaunal benthic foraminifera has been used as a proxy for surface productivity through benthic-pelagic coupling, we argue that this proxy can be used only in the absence of changes in carbonate saturation and current-driven biophysical linking.

1. Introduction

The late Paleocene through early Eocene greenhouse world started to warm in the late Paleocene, culminating the warmest part of the Cenozoic during the Early Eocene Climate Optimum, followed by gradual cooling of high latitudes and deep-sea waters from the end of the early Eocene on Zachos *et al.* [2001, 2008]. This long-term evolution was punctuated by short, extreme warming events called hyperthermals [Thomas *et al.*, 2000; Thomas and Zachos, 2000; Cramer *et al.*, 2003; Zachos *et al.*, 2010; Leon-Rodriguez and Dickens, 2010; Littler *et al.*, 2014]. During such events, large amounts of isotopically light carbon were released rapidly into the ocean-atmosphere system [Dickens *et al.*, 1995, 1997], causing negative carbon isotope excursions (CIEs) in carbonate and organic matter, coeval with oxygen isotope excursions indicative of warming, and dissolution of calcium carbonate [Cramer *et al.*, 2003; Zachos *et al.*, 2010].

The Paleocene-Eocene Thermal Maximum (PETM, ~55.5 Ma) was the most extreme of these hyperthermals, characterized by a 5–8°C increase in global temperatures [Zachos *et al.*, 2003; Sluijs *et al.*, 2007; McInerney and Wing, 2011; Dunkley Jones *et al.*, 2013], a negative CIE of at least ~2.5‰ and possibly up to 4.5‰ [Kennett and Stott, 1991; Thomas and Shackleton, 1996; McCarren *et al.*, 2008; Handley *et al.*, 2008], ocean acidification of the surface ocean [e.g., Penman *et al.*, 2014], shoaling of the calcite compensation depth (CCD) and carbonate dissolution on the seafloor [Zachos *et al.*, 2005], perturbation of the hydrological cycle [Pagani *et al.*, 2006; Eldrett *et al.*, 2014], and possibly regional deoxygenation of sea bottom waters [Chun *et al.*, 2010; Pälike *et al.*, 2014] and expanding Oxygen Minimum Zones [Zhou *et al.*, 2014]. Carbon cycling within the oceans, specifically the depth of remineralization of organic matter, may have changed during the warming [Ma *et al.*, 2014; John *et al.*, 2013, 2014], and open ocean productivity may have declined [e.g., Winguth *et al.*, 2012]. Perturbation of biotic assemblages on land and in the oceans [McInerney and Wing, 2011], including the largest extinction of deep-sea benthic foraminifera of the Cenozoic [Thomas, 2007], is among the consequences of the PETM, as are migrations of biota

Table 1. Eocene Hyperthermal Events

Hyperthermal Events	Age (Ma)	References
Paleocene-Eocene Thermal Maximum (PETM or ETM1)	55.5	<i>Kennett and Stott [1991], Thomas and Shackleton [1996], and Zachos et al. [2003, 2005]</i>
Eocene Thermal Maximum-2 (ETM2, also called ELMO or H1)	53.7	<i>Lourens et al. [2005], Sluijs et al. [2009], Galeotti et al. [2010], Leon-Rodriguez and Dickens [2010], and Stap et al. [2009, 2010]</i>
H2	53.6	<i>Cramer et al. [2003] and Stap et al. [2009, 2010]</i>
I1	53.2	<i>Cramer et al. [2003] and Leon-Rodriguez and Dickens [2010]</i>
Eocene Thermal Maximum-3 (ETM3 or X event)	52.5	<i>Cramer et al. [2003], Röhl et al. [2005], Agnini et al. [2009], Galeotti et al. [2010], and Leon-Rodriguez and Dickens [2010]</i>
C22r-H1 to H3, C22n-H1 and H2, and C21r-H1 to H5	50–48.2	<i>Sexton et al. [2011]</i>
C21r-H6	47.44	<i>Sexton et al. [2011] and Payros et al. [2012]</i>
C19r	41.8	<i>Edgar et al. [2007]</i>
MECO	40.6–40	<i>Bohaty and Zachos [2003] and Bohaty et al. [2009]</i>

to higher latitudes on land and in the oceans [e.g., *McInerney and Wing, 2011; Speijer et al., 2012*]. Other hyperthermals, similar to the PETM but of lesser magnitude, are less well documented (Table 1). In addition, at ~40 Ma the middle Eocene Climate Optimum (MECO) interrupted the deep water and high-latitude cooling trend starting at the end of the early Eocene [*Bohaty and Zachos, 2003; Bohaty et al., 2009*]. The MECO had a longer duration than earlier hyperthermals, with peak warming not clearly associated with a CIE [*Bohaty et al., 2009; Sluijs et al., 2013; Boscolo-Galazzo et al., 2014*].

Many hyperthermals have been described only by fluctuations in proxies for temperature using $\delta^{18}\text{O}$, carbonate/terrigenous content or $\delta^{13}\text{C}$ in bulk carbonates, or benthic foraminifera, and their occurrence at orbital frequencies highlighted [*de Conto et al., 2012; Payros et al., 2012; Littler et al., 2014; Lauretano et al., 2015*], although the PETM has been suggested to be out of phase with other hyperthermals [*Cramer et al., 2003; Zachos et al., 2010*]. Biotic effects of other hyperthermals, such as the Eocene Thermal Maximum 2 (ETM2) or Eocene Thermal Maximum 3 (ETM3), have been described in much less detail and from fewer localities than the PETM [e.g., *Agnini et al., 2009; d'Haenens et al., 2012; Jennions et al., 2015*]. As an example, the deep-sea benthic foraminiferal turnover across the PETM has been intensely studied over the past decades [e.g., *Thomas, 1998, 2003, 2007; Alegret et al., 2009a, 2009b, 2010*], but there are few studies dealing with the turnover across the ETM2 [*d'Haenens et al., 2012; Jennions et al., 2015*] and the ETM3 [*Röhl et al., 2005*], and they are all based on sites in the Atlantic Ocean. Therefore, the characteristics of the various Eocene hyperthermals and specifically their effects on the biota are not well known yet, but they share features with the PETM such as global warming, negative CIEs, carbonate dissolution, biotic perturbations, and increased continental weathering [e.g., *Thomas and Zachos, 2000; Nicolo et al., 2007; Stap et al., 2010; Lauretano et al., 2015*].

Because of the similarities among the hyperthermals, it is widely accepted that they may have had a common cause, i.e., emission of isotopically light carbon compounds to the ocean-atmosphere system. The source of the carbon compounds as well as the triggering mechanism of emission are still under strong debate, including such diverse proposed sources as methane from dissociation of gas hydrates through oceanic warming [e.g., *Dickens et al., 1995; Dickens, 2011*] possibly triggered through orbital forcing [*Lunt et al., 2011*], release of carbon from organic matter oxidation through drying of marginal basins [*Higgins and Schrag, 2006*], burning of peat deposits [*Kurtz et al., 2003*], heating of organic matter by intrusion of volcanic sills [*Svensen et al., 2004, 2010; Storey et al., 2007*], release of dissolved methane from a silled North Atlantic Basin [*Nisbet et al., 2009*], and orbitally forced dissociation of permafrost deposits on Antarctica [*de Conto et al., 2012*].

Seamounts are geographically isolated topographic features rising > 100 m above the surrounding seafloor [*Staudigel et al., 2010*], where interaction of geological, oceanographic, and biological factors [*Genin, 2004*] creates unusual ecological settings, commonly characterized by high biodiversity [*McClain, 2007; Shank, 2010*]. Because of their geographic isolation, some authors consider the occurrence of endemic species typical [e.g., *de Forges et al., 2000*], whereas others argue that the observed percentage of endemism may be biased by sampling problems [*McClain, 2007; McClain et al., 2009*] or that the interaction of currents does not affect the efficiency of larval dispersion [*Samadi et al., 2006*]. Benthic foraminifera are characterized by a motile life stage (propagules) [*Alve and Goldstein, 2003, 2010*], and genetic information on a few deep-sea species suggests that they are cosmopolitan [*Pawlowski et al., 2007; Burkett et al., 2015*], thus

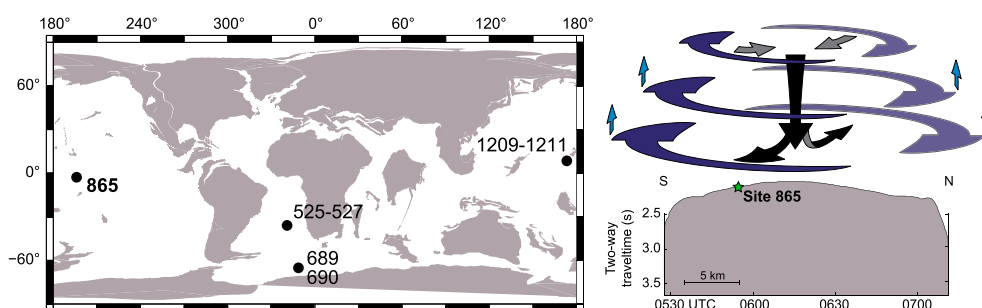


Figure 1. Palaeogeographic reconstruction at 55.5 Ma, modified from Hay *et al.* [1999], showing all sites mentioned in text, and cross section of Allison Guyot (ODP Site 865), modified from Sager *et al.* [1993]. The arrows show a schematic diagram of the current system over seamounts, according to Mullineaux and Mills [1997].

highly efficient dispersers. Studies on recent assemblages from seamounts have not documented endemic benthic foraminiferal species [e.g., Heinz *et al.*, 2004], although abyssal species inhabiting elevated objects on the seafloor appear to differ between ocean basins [Gooday *et al.*, 2015].

Around the steep, abrupt seamount topography, currents are intensified, including eddies and circular currents around the upper part of the seamount [Lavelle and Mohn, 2010]. These currents not only winnow fine particles including organic matter, thus removing food from benthic communities [e.g., Heinz *et al.*, 2004], but also trap organisms and food particles in some parts of the seamount in a process called “trophic focusing,” resulting in rich, sometimes highly localized concentrations of biota [Genin *et al.*, 1998; Genin, 2004]. Importantly, effects of the current activity (biophysical coupling) [Dower and Brodeur, 2004] around seamounts may break the link between primary productivity in surface waters and arrival of food on the seafloor (benthic-pelagic coupling). Food particles may be either swept away or concentrated, dependent upon location on the seamount top, so that locally more or less food arrives at the seafloor than calculated from primary productivity through application of a logarithmic transfer equation [e.g., Martin *et al.*, 1987]. A seamount setting thus adds additional complexity to the process of transfer of organic matter to the seafloor, a process now realized to be much more complex than envisaged in the 1990s, with the transfer equation highly dependent upon pelagic ecosystem structure [Boyd and Trull, 2007; Henson *et al.*, 2012]. In addition, transfer efficiency may vary during periods of climate change as a consequence of differentially changing metabolic rates of different participants of the food chain [Ma *et al.*, 2014; John *et al.*, 2013, 2014].

Seamount top ecosystems are commonly dominated by suspension feeders [e.g., Genin *et al.*, 1998]. Meiofauna (including benthic foraminifera) may be reworked on the top of the seamount [Thistle *et al.*, 1999; Wilson and Boehlert, 2004], and strong near-bottom flow may result in reduced abundance [Thistle and Levin, 1998]. The few studies on seamount foraminifera suggest that their distribution and diversity are indeed dominantly controlled by currents [Kustanowich, 1962; Nienstedt and Arnold, 1988; Ohkushi and Natori, 2001; Heinz *et al.*, 2004; García-Muñoz *et al.*, 2012], whereas food supply linked to primary productivity is generally seen as the main determinant of deep-sea benthic foraminiferal faunas, when oxygen availability is not a critical factor, which it becomes only at extremely low levels (~ 0.1 ml/L) [e.g., Jorissen *et al.*, 1995, 2007; Murray, 2001; Gooday, 2003].

In order to compare the biotic turnover across the PETM and less intense hyperthermal events at a location distal from the Atlantic Ocean, we document the long-term, late Paleocene to middle Eocene evolution of benthic foraminifera on a seamount in the Mid-Pacific mountain chain and evaluate the effects of long-term climate change and superimposed, short-term hyperthermal events in this unusual setting.

2. Setting of Site 865

Paleocene-middle Eocene pelagic sediments overlying the top of Allison Guyot in the equatorial Pacific ($18^{\circ}26'N$, $179^{\circ}33'W$, 1530 m present water depth; Figure 1) were recovered during Ocean Drilling Program Leg 143 at Site 865. We studied Cores 865B-3H to 865B-15X (upper Paleocene and Eocene) and included material from Core 865C-12H (uppermost Paleocene) because the PETM occurred in a core break [Bralower *et al.*, 1995a, 1995b]. These cores were recovered by hydraulic piston corer, with the exception of Core 865B-15X, recovered with the extended core barrel. The correlation between cores from the two holes follows Bralower *et al.* [1995a, 1995b].

The studied interval consists of about 116 m of pale yellow-white foraminiferal-nannofossil ooze with burrow mottles with nannofossil ooze infill and sporadic small black specks toward the base of the studied interval. The carbonate content is uniformly high, between 92 and 98% [Sager *et al.*, 1993]. Planktonic foraminifera, the main component of the sand-sized fraction, are strongly enriched over finer particles through winnowing by bottom currents [Sager *et al.*, 1993; Bralower *et al.*, 1995a], as seen in the high values of weight percent of coarse fraction (CF; $>63\ \mu\text{m}$) [Yamaguchi and Norris, 2015]. Cores 865B-1H through the middle part of 865B-3H (depth in hole ~ 0 –19.2 meters below seafloor (mbsf)) contain strongly mixed material from various ages, including Neogene and Paleogene species and thus were excluded from this study [Bralower *et al.*, 1995a].

Below this interval, the record is almost complete for the time between about 60 and 38.5 Ma (upper Paleocene through middle Eocene), except for an unconformity over the interval corresponding to ~ 49 –51.5 Ma (depth in hole ~ 79.20 –80.70 mbsf). The record across the peak PETM is condensed [Bralower *et al.*, 1995a, 1995b; Kelly *et al.*, 1996, 1998; Nunes and Norris, 2006], and there is considerable evidence for sediment mixing through bioturbation and/or coring disturbance, as seen in the $\delta^{13}\text{C}$ signature of single specimens of planktic foraminifera [e.g., Kelly *et al.*, 1996, 1998]. The paleodepth of Site 865 was estimated as upper lower bathyal (~ 1300 –1500 m), and it was at a paleolatitude ranging from about 2°N in the Paleocene to 6°N in the late Eocene [Bralower *et al.*, 1995a]. Calcareous nannofossil biostratigraphy was evaluated by Bralower and Mutterlose [1995]. Planktic foraminifera underwent rapid evolution across the PETM, with the so-called “excursion taxa” (e.g., *Morozovella allisonensis*, *M. africana*, and *Acarinina sibaiyaensis*) indicating changes in water column stratification and declining productivity, the latter supported by nannofossil evidence for intensified oligotrophy in an already oligotrophic setting [Kelly *et al.*, 1996, 1998]. I/Ca values of planktic foraminifera confirm that Site 865 was strongly oligotrophic [Zhou *et al.*, 2014]. Benthic ostracodes were studied at low resolution by Boomer and Whatley [1995], in more detail by Yamaguchi and Norris [2015], showing significant extinction. In contrast to the planktic records [Kelly *et al.*, 1996], benthic foraminiferal assemblages have been interpreted as reflecting increased arrival of food at the seafloor [Thomas, 1998; Thomas *et al.*, 2000].

Planktic and benthic foraminiferal stable isotope stratigraphy was documented by Bralower *et al.* [1995a, 1995b], with additional benthic stable isotope data included in Thomas *et al.* [2000] and Katz *et al.* [2003]. The long-term planktic and benthic foraminiferal oxygen isotope records [Bralower *et al.*, 1995a, 1995b] show an increase from the end of the early Eocene on, interpreted as reflecting global cooling at this low-latitude site. Later evaluation documented extensive recrystallization of the planktic foraminifera on the seafloor [Pearson *et al.*, 2001], indicating that high latitudes and deep waters cooled, while tropical temperatures remained high [Pearson *et al.*, 2007].

Mg/Ca data on benthic foraminiferal tests across the PETM show bottom water warming of about 3 – 4°C [Tripathi and Elderfield, 2005]. Stable isotope ($\delta^{18}\text{O}$) data for planktic foraminifera across the PETM were interpreted to indicate minor surface water warming [Bralower *et al.*, 1995a, 1995b] but later recognized to have been affected by diagenesis on the seafloor [Pearson *et al.*, 2001; Kozdon *et al.*, 2011, 2013; Dunkley Jones *et al.*, 2013; Edgar *et al.*, 2015]. Detailed analysis of nonrecrystallized parts of the planktic tests indicates that sea surface temperatures increased by about 5°C or more during the PETM, reaching at least 33°C [Kozdon *et al.*, 2011, 2013].

Diagenetic effects were more severe within the PETM interval, supporting the occurrence of carbonate dissolution followed by reprecipitation, as suggested by the presence of large euhedral calcite crystals encompassing planktic foraminifera [Kozdon *et al.*, 2013] (Figure S1 in the supporting information). Due to the lack of fine-grained terrestrial material, CaCO_3 dissolution during the PETM may not have resulted in formation of a clay layer, and CaCO_3 weight percent remained high in the interval with dissolution/reprecipitation across the PETM. The observation that dissolution-recrystallization occurred during the PETM but not at other intervals indicates that the lysocline was shallower than the paleodepth of Site 865, even though carbonate dissolution was less severe in the Pacific than in the Southeast Atlantic [Colosimo *et al.*, 2005; Zachos *et al.*, 2005].

Despite the problems in the stable isotope record of Site 865, negative $\delta^{13}\text{C}$ excursions mark the PETM and ETM3 [Bralower *et al.*, 1995a; Thomas *et al.*, 2000; Zachos *et al.*, 2001], although the most extreme values of the isotope excursions, as determined by analysis of multiple specimens, remain below the extreme values as seen in single-specimen analysis [Kelly *et al.*, 1996]. The probability of not resolving a smaller excursion thus is greater than that of resolving a larger excursion, and the probability of resolving an excursion becomes lower at lower sedimentation rates [Kirtland-Turner and Ridgwell, 2014].

Neither the ETM2 nor the MECO was recognized in the stable isotope records at the resolution of our study, probably because of a combination of bioturbation and coring disturbance, at overall low sedimentation rates. The MECO interval occurs within Cores 865B-3H and 865B-4H, at the upper boundary of the level where sediments are largely stratigraphically intact (Cores 865B-3H and lower), whereas the upper two cores in the hole contain sediment that is fully mixed, probably due to very low sedimentation rates [Bralower *et al.*, 1995a]. However, the two samples analyzed across the MECO are within an interval that might have been affected by bioturbation more strongly than older material (Figure S2). The photograph of Core 865B-11H (Figure S3) shows bioturbation in the intervals above (section 3, 110 cm and upward) and possibly immediately below our sample 11H-1, 120–125 cm. This sample is correlated with the ETM2, but due to uncertainties in our age model, the hyperthermal event might occur at a slightly different level and thus fall within a bioturbated interval. In contrast, samples studied across the PETM and ETM3 were picked from intervals considerably less affected by bioturbation as observed in the sediments (Figures S4 and S5) due to higher sedimentation rates. Our sampling resolution is low (Figures S2–S5 and Table S1), and therefore, mild bioturbation would not affect our benthic foraminiferal results significantly.

The main aspects of the benthic foraminiferal turnover across the PETM at Allison Guyot were first described by Thomas [1998] and Thomas *et al.* [2000], but no detailed information was provided, and the assemblage turnover across the ETM3 and MECO has not been documented. Later, cylindrical taxa with complex apertures were studied by Hayward *et al.* [2012]. Here we document for the first time the late Paleocene to Eocene benthic foraminiferal assemblages from this Pacific seamount and look into faunal turnover across hyperthermal events.

3. Methods

A set of 97 samples were analyzed, covering the upper Paleocene (planktic foraminiferal zones P3b–P5, calcareous nannofossil zones NP4–NP9) through lower middle Eocene (P5–P15, NP9–NP18; Figure S6). The sampling resolution varied between 2 cm (in the intervals of expected hyperthermals) and 1.5 m (one sample per core section). Samples were oven-dried at 60°C, soaked in warm water with detergent, and wet sieved over a 63 μm sieve. Samples were weighed before and after sieving to determine the weight percent of the coarse fraction (CF%) in order to evaluate winnowing (thus probably current intensity) over time. Coarse fraction weight percent is considered a proxy for winnowing on top guyot settings, because sediments deposited under these hydrographic conditions tend to experience winnowing by bottom currents both during deposition and shortly thereafter [Bralower and Mutterlose, 1995].

Quantitative analyses of benthic foraminiferal assemblages were based on 300 individuals per sample from the $>63 \mu\text{m}$ size fraction (Table S1) and allowed us to infer such parameters as paleodepth, bottom current velocity, oxygen concentration of the bottom waters, and the quantity and quality of organic matter reaching the seafloor [Jorissen *et al.*, 2007]. We followed the generic classification by Loeblich and Tappan [1987] as modified by Hayward *et al.* [2012] for uniserial taxa with complex apertures and Tjalsma and Lohmann [1983], van Morkhoven *et al.* [1986], Alegret and Thomas [2001], and Hayward *et al.* [2012] for determinations at the species level (Figure S7). The relative abundance of selected species and morphological suprageneric groups (Tables 2, S2, and S3) was used to infer the paleoenvironmental turnover across the studied events. Suprageneric groups include cylindrical taxa with complex apertures (with rectilinear, generally uniserial tests), buliminids and bolivinids *sensu stricto* (s.s.) and buliminids *sensu lato* (s.l.). The group buliminids s.s. only includes genera of the superfamily Buliminacea, and the wider group buliminids s.l. includes genera of the superfamilies Buliminacea, Bolivinacea, Loxostomatacea, Turritellacea, and Pleurostomellacea [Sen Gupta, 1999].

The relative abundance of the infaunal buliminid group was calculated, as this group of detrital feeders tolerates reduced oxygen concentrations [Sen Gupta and Machain-Castillo, 1993] and/or thrives under an abundant food supply [Thomas, 1998; Fontanier *et al.*, 2002; Gooday, 2003; Jorissen *et al.*, 1995, 2007] in modern oceans. All species were allocated into habitat-related morphogroups (infaunal versus epifaunal; Table S4), which in general can be used as proxies for oxygenation and trophic conditions at the seafloor, with high relative abundance of infaunal taxa thought to be indicative of a high food supply and/or low oxygen availability [e.g., Jorissen *et al.*, 1995, 2007]. However, this parameter must be used with caution, because even for many living taxa the relation between morphology and microhabitat has not been well established [e.g., Jorissen, 1999], and assignments may be correct only about 75% of the times [Buzas *et al.*, 1993].

Table 2. Benthic Foraminifera Mentioned in the Text, Including Some of Their Ecological Preferences and Paleoenvironmental Implications

Group	Selected Species	Test	Life Position	Ecological Preferences/Paleoenvironmental Implications
	Abyssaminids	Calcareous	Infaunal	Oligotrophy, opportunistic ^a
	<i>Cibicidoides</i> spp.	Calcareous	Epifaunal	Increased bottom current activity ^{b,c}
	<i>Gyroidinoides</i> spp.	Calcareous	Epifaunal	Opportunistic, meso-oligotrophic environments ^d
	Lenticulinids	Calcareous	Shallow infaunal	Resistant to dissolution ^e
	<i>Nuttallides truempyi</i>	Calcareous	Epifaunal	Oligotrophy, tolerant to corrosive waters ^f
	<i>Nuttallides umbonifera</i>	Calcareous	Epifaunal	Oligotrophy, tolerant to corrosive waters ^f
	<i>Oridorsalis umbonatus</i>	Calcareous	Infaunal	Oxic, low-sustained flux of degraded organic matter ^g
	<i>Stens. beccariiiformis</i>	Calcareous	Epifaunal	High food supply ^{h,i}
Boliviniids s.s.	<i>Bolivinioides decoratus</i>	Calcareous	Infaunal	Abundant food supply and/or low oxygenation ^{i,f,k}
	<i>Tappanina selmensis</i>	Calcareous	Infaunal	Abundant food supply and/or low oxygenation ^{i,f,k}
Buliminids s.s.	<i>Bulimina semicostata</i>	Calcareous	Infaunal	High food environments ^{k,h}
	<i>Bulimina simplex</i>	Calcareous	Infaunal	High food environments ^{k,h}
	<i>Buliminella beaumonti</i>	Calcareous	Infaunal	High food environments ^{k,h}
	<i>Quadratobul. pyramidalis</i>	Calcareous	Infaunal	High food environments ^{k,h}
	<i>Siphogen. brevispinosa</i>	Calcareous	Infaunal	High food environments ^{k,h}
Buliminids s.l.	<i>Aragonia aragonensis</i>	Calcareous	Infaunal	Opportunistic, potential marker of hyperthermals ^{l,m,n}
	<i>Globocassid. subglobosa</i>	Calcareous	Infaunal	Oxic, pulsed food input, fresh phytodetritus ^{k,o}
	Pleurostomellids	Calcareous	Infaunal	High food supply ^b
	<i>Pyramidina rudita</i>	Calcareous	Infaunal	Opportunistic, high food supply ^{i,c}
Cylindrical taxa	<i>Stilostomella</i> spp.	Calcareous	Infaunal	Resistant to enhanced current activity ^c
	<i>Strictocostella</i> spp.	Calcareous	Infaunal	Resistant to enhanced current activity ^c
Uniserial lagenids	Nodosariids	Calcareous	Infaunal	High food supply ^b

^aThomas [2007];^bThomas et al. [2000];^cThis study;^dSchmiedl et al. [2003];^eNguyen et al. [2009];^fThomas [1998];^gMackensen et al. [1995];^hAlegret and Thomas [2009];ⁱAlegret and Thomas [2005];^jSen Gupta and Machain-Castillo [1993];^kJorissen et al. [2007];^lSteineck and Thomas [1996];^mAlegret et al. [2009a];ⁿOrtiz et al. [2011];^oSmart et al. [2007].

The Fisher- α diversity index and the Shannon-Weaver heterogeneity index were calculated. The former correlates the number of species and the number of individuals in each sample [Murray, 2006], and the latter depends on the relative abundance and the number of taxa [Hammer and Harper, 2006]. The benthic foraminiferal accumulation rate (BFAR), i.e., the number of benthic foraminifera per square centimeter per thousand years, is a proxy for export productivity, with higher numbers indicating more organic carbon reaching the seafloor [Herguera and Berger, 1991; Jorissen et al., 2007]. BFARs were calculated using data on dry bulk density [Sager et al., 1993] and data on CF% and the number of foraminifera per gram. BFARs have been used extensively to estimate the flux of food to the seafloor [Herguera and Berger, 1991; Jorissen et al., 2007]. We can, however, not assume that BFARs on seamounts reflect primary productivity in the surface waters, in contrast with, e.g., the region studied by Herguera and Berger [1991] to define BFAR, because of the potential biophysical coupling of food supply to current regime [e.g., Genin, 2004].

The age model is mainly based on the calcareous nannofossil stratigraphy [Bralower and Mutterlose, 1995; Bralower et al., 1995a, 1995b]. We used the biostratigraphic datum levels in Bralower et al. [1995a], recalculated ages to the modern time scale as in Yamaguchi and Norris [2015], but our age scale differs from that in these authors by placing the base of the PETM at 55.5 Ma. We then fine-tuned the biostratigraphy through correlation of the stable isotope stratigraphy with that of Littler et al. [2014]. We overlaid the low-resolution record from Site 865 over the high-resolution record in Littler et al. [2014] then minimized the differences between the low-resolution curve and a 7 pt moving average of the Littler et al. [2014] curve. Numerical age values for all samples are shown in Table S1.

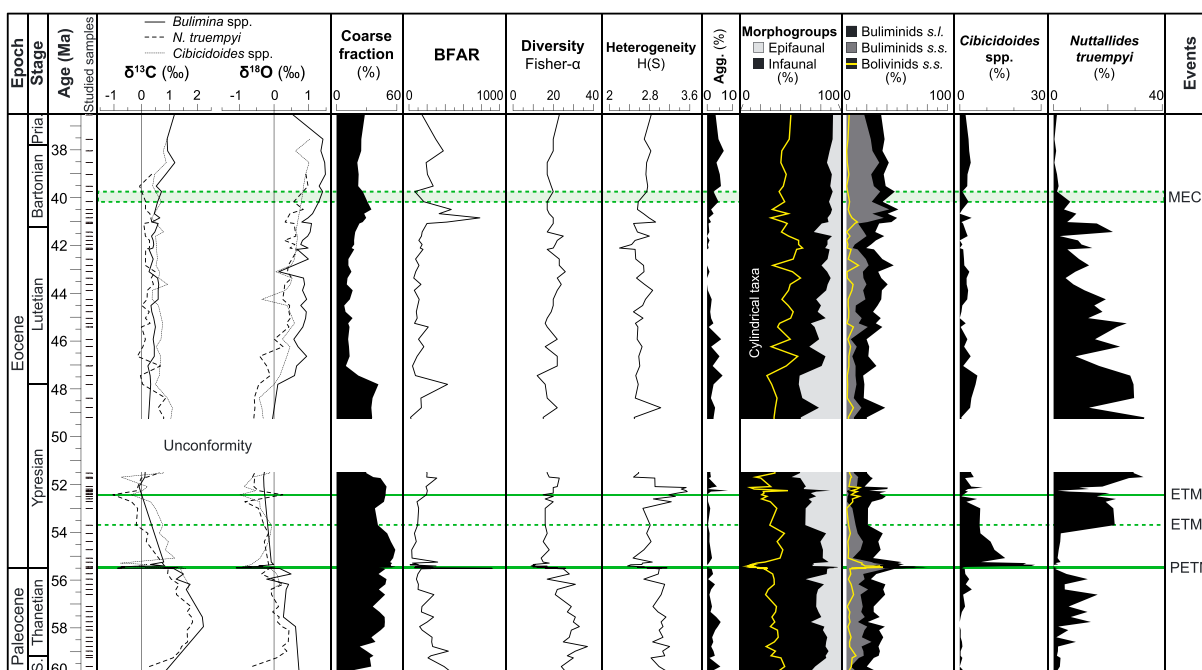


Figure 2. $\delta^{13}\text{C}$ and $\delta^{18}\text{O}$ values in benthic foraminiferal species across the upper Paleocene-middle Eocene at ODP Site 865, shown with weight percent coarse fraction (CF%), benthic foraminiferal accumulation rates (BFAR), diversity and heterogeneity indices, percentages of agglutinated taxa, infaunal-epifaunal morphogroups, cylindrical taxa, buliminids s.l., buliminids s.s., boliviniids s.s., *Cibicidoides* spp., and *Nuttallides truempyi*. See Table S2 for genera included in each morphological group; calcareous/agglutinated genera are shown in Table S3 and infaunal/epifaunal species in Table S4. Stable isotope data are from Bralower *et al.* [1995a, 1995b] and Katz *et al.* [2003]. Abbreviations: H(S), Heterogeneity (Shannon-Weaver).

4. Results

The weight percent coarse fraction (CF%) ranges between 10 and 60% (Figure 2), with higher values in the uppermost Paleocene-lowermost Eocene (between 47.8 and 59.9 Ma) and a marked drop at about 47.8 Ma, followed by a slight increase between 43 and 40 Ma, i.e., before the MECO. Low values in the lowermost two samples cannot be evaluated due to poor preservation. The CF% is negatively correlated with benthic foraminiferal $\delta^{18}\text{O}$ values (Figures 2–4).

In contrast to planktic foraminifera, which lived in surface waters, the benthic foraminiferal specimens, which secrete their tests in deep waters and have much less porous walls than planktics, are well preserved, the ornamentation of their tests (e.g., spines) is clearly recognized, and they show no evidence for significant recrystallization. Benthic foraminiferal assemblages at Site 865 are diverse and heterogeneous (Figure 2). Agglutinated foraminifera and lenticulinids, a dissolution-resistant group, make up less than 9% and 11% of the assemblages, respectively (Table S1 and Figure S8). Assemblages are dominated by infaunal morphogroups (mean values ~80%), including buliminids s.l. and cylindrical taxa with complex apertures, generally dominated by species of the genera *Strictocostella* and *Siphonodosaria* (Figure 2) that are included in the group Stilostomellidae [Hayward *et al.*, 2012, Appendix 16]. Overall, BFAR values are low across the studied interval, and the most prominent, positive peaks are recorded within the PETM, coinciding with high percentages of buliminid taxa (Figure 5) and below the MECO (Figure 2). Among epifaunal taxa, *Cibicidoides* spp. are common in the lowermost Eocene and *Nuttallides truempyi* in the upper Ypresian-lower Lutetian (Figure 2). The assemblages gradually decrease in diversity and heterogeneity in the uppermost Paleocene and decline markedly at the Paleocene/Eocene boundary during the benthic extinction event (BEE). Diversity indices only show a very minor decrease across the ETM3 and no significant variations in the interval where the MECO should be located (Figure 2).

Paleocene assemblages are diverse and dominated by infaunal taxa such as buliminids s.s., boliviniids s.s., and cylindrical taxa (Figure 2), mainly stilostomellids, with *Strictocostella pseudoscripta/spinata* as the most common species [Hayward *et al.*, 2012].

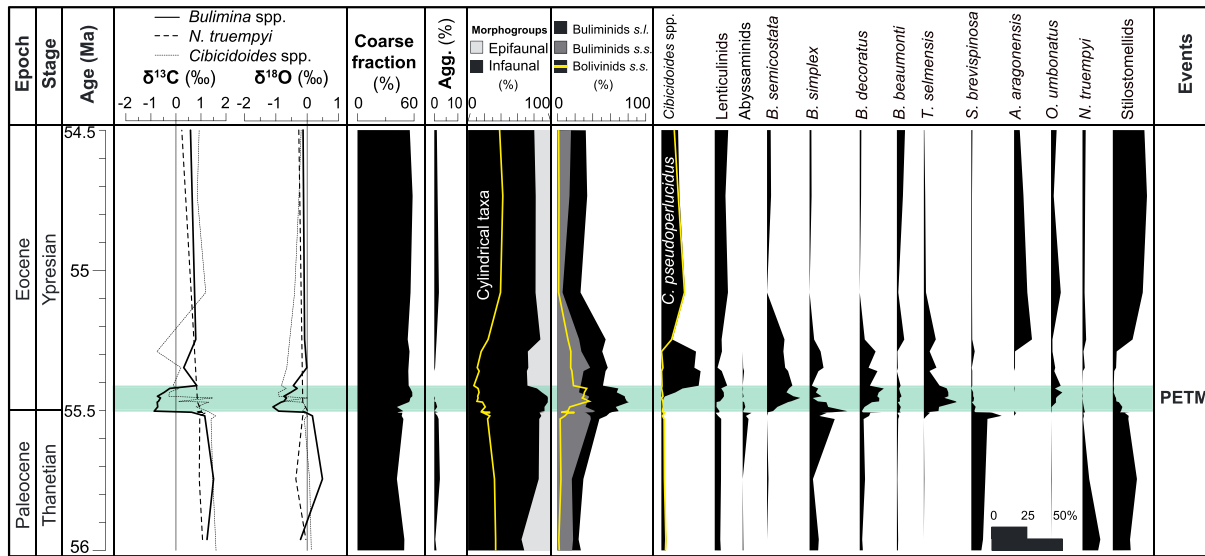


Figure 3. $\delta^{13}\text{C}$ and $\delta^{18}\text{O}$ values in benthic foraminiferal species across the PETM at the ODP Site 865. Percentages of agglutinated taxa, infaunal-epifaunal morphogroups, cylindrical taxa, buliminids s.l., buliminids s.s., and bolivinids s.s. Relative abundance of selected benthic foraminiferal taxa and percentage of coarse fraction. Stable isotope data from Bralower et al. [1995a, 1995b] and Katz et al. [2003].

The turnover across the BEE is marked by the extinction of 10.4% of species and the local/regional last occurrence of 22.9% of species (Table S5). Agglutinated taxa are almost absent across the PETM (Figures 2 and 3). Infaunal taxa, such as buliminids s.s. (e.g., *Bulimina semicostata*, *B. simplex*) and bolivinids s.s. (e.g., *Bolivinoides decoratus*, *Tappanina selmensis*), sharply increased in relative abundance across the peak CIE. The cylindrical taxa temporarily

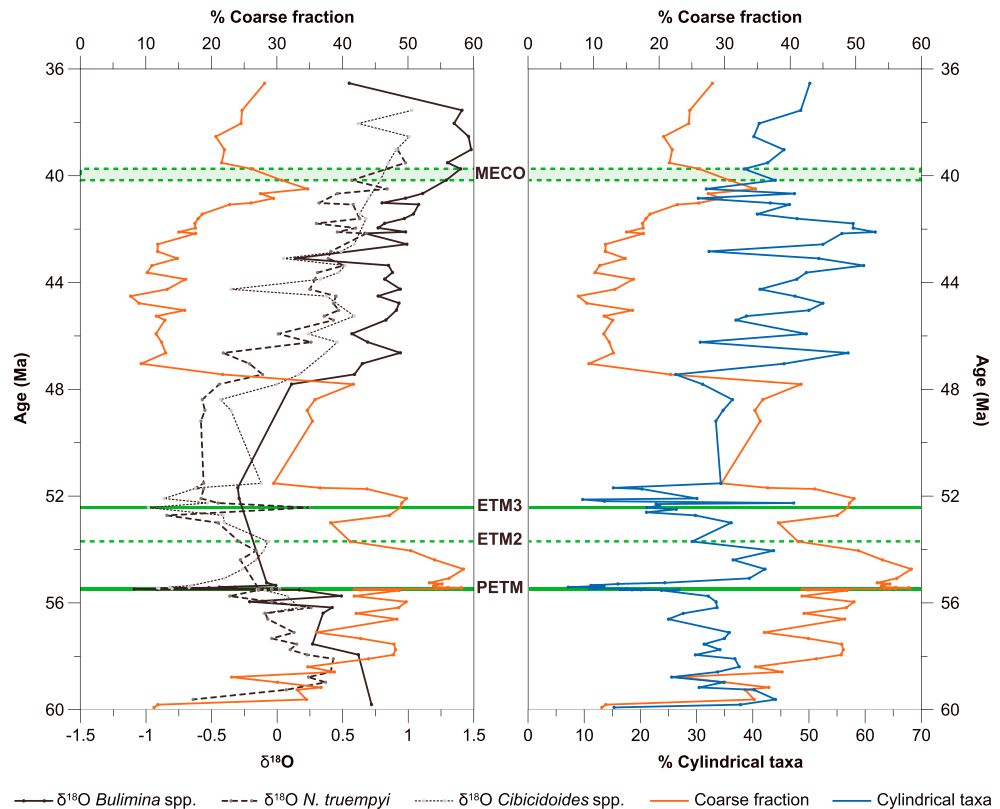


Figure 4. $\delta^{18}\text{O}$ values versus weight percent coarse fraction (CF%) and coarse fraction versus relative abundance of cylindrical taxa. Stable isotope data from Bralower et al. [1995a, 1995b] and Katz et al. [2003].

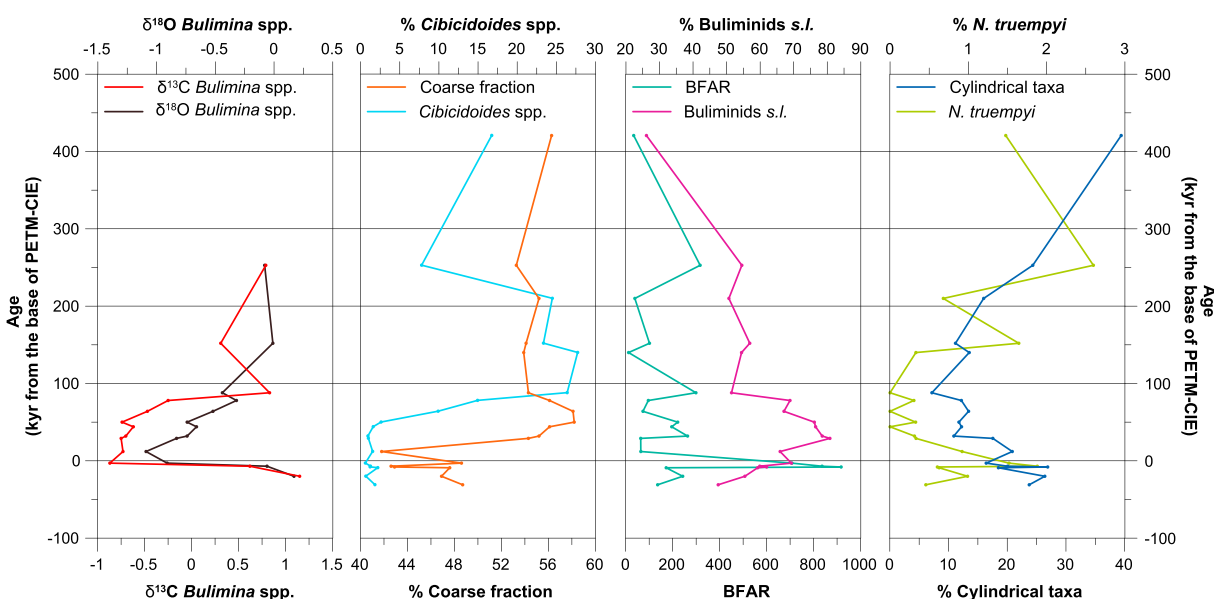


Figure 5. $\delta^{13}\text{C}$ versus $\delta^{18}\text{O}$ values, relative abundance of *Cibicidoides* species versus coarse fraction, BFARs versus percentage of buliminids, and percentages of cylindrical taxa and *N. truempyi* across the PETM interval. Stable isotope data from Bralower et al. [1995a, 1995b] and Katz et al. [2003].

declined in abundance (Figure 3), especially the spinose stilostomellids, but the percentage of smooth-walled pleurostomellids (Figure S8) increased [Hayward et al., 2012]. The whole group of cylindrical taxa with complex apertures did not show significant net extinction during the PETM [Hayward et al., 2012]. The epifaunal *N. truempyi* is very rare immediately above the extinction event, and the few specimens present have a pre-extinction carbon isotope signature and thus were bioturbated into the lower Eocene [Bralower et al., 1995a, 1995b]. The shallow infaunal buliminids show the clear signature of the PETM CIE [Zachos et al., 2001]. Large, flat *Cibicidoides* species peak in relative abundance above the CIE, but specimens with a CIE stable isotope signature occur right below the base of the CIE and thus are probably bioturbated or brought to that level by coring disturbance.

Overall, BFARs increased across the PETM but show large fluctuations. The CF% fluctuated during the first ~20,000 years (kyr) of the event and increased 60 kyr after the P/E boundary coeval with the initial recovery of $\delta^{13}\text{C}$ values in benthic foraminifera, a gradual decrease in the percentage of buliminids s.l. and an increase in relative abundance of large discoidal *Cibicidoides* (Figure 5).

Lower Eocene assemblages (between ~55 and 52.5 Ma) contain slightly higher percentages of dissolution-resistant forms such as lenticulinids and *Oridorsalis umbonatus*, as well as common *Cibicidoides* species and opportunistic taxa such as *Aragonia aragonensis* (Figures 3 and S8). The percentage of *Cibicidoides* spp. gradually decreased across this interval, and cylindrical taxa recovered their pre-PETM abundance values.

Low sedimentation rates preclude identification of the ETM2, but a prominent increase in relative and absolute abundance of *N. truempyi* at ~53.7 Ma coincided with or just postdated this event. The identification of ETM3 at Site 865 is based on low $\delta^{13}\text{C}$ values in *Cibicidoides* and *N. truempyi* (Figures 2 and 6). No significant extinctions have been recorded across this event (Table S5), but faunal changes include a slight increase in the percentage of buliminids s.l. (Figure 2) and an abundance peak of *A. aragonensis* (Figure 6).

The lower percentage of cylindrical taxa (stilostomellids and uniserial lagenids) and agglutinated taxa increased ~170 kyr after the ETM3, coinciding with a sharp decrease in *N. truempyi* and a slight decrease in the percentage of buliminids s.l. The relative abundance of buliminids s.l., *Cibicidoides* spp., *B. decoratus*, *Globocassidulina subglobosa*, *Nuttallides umbonifera*, *Pyramidina rudita*, and *Gyroidinoides* spp. increased ~238 kyr after ETM3, coeval with a decrease in relative abundance of cylindrical taxa (Figure 6).

The relative abundance of *N. truempyi* decreased markedly in the upper half of the studied interval (~51.5–36.5 Ma), coeval with an increasing trend in buliminids s.l. and cylindrical taxa (Figures 2 and S8), which are largely dominated by the species most abundant throughout the studied interval, *Strictocostella pseudoscripta* [Hayward et al., 2012]. A prominent decrease in CF% occurred at ~47 Ma.

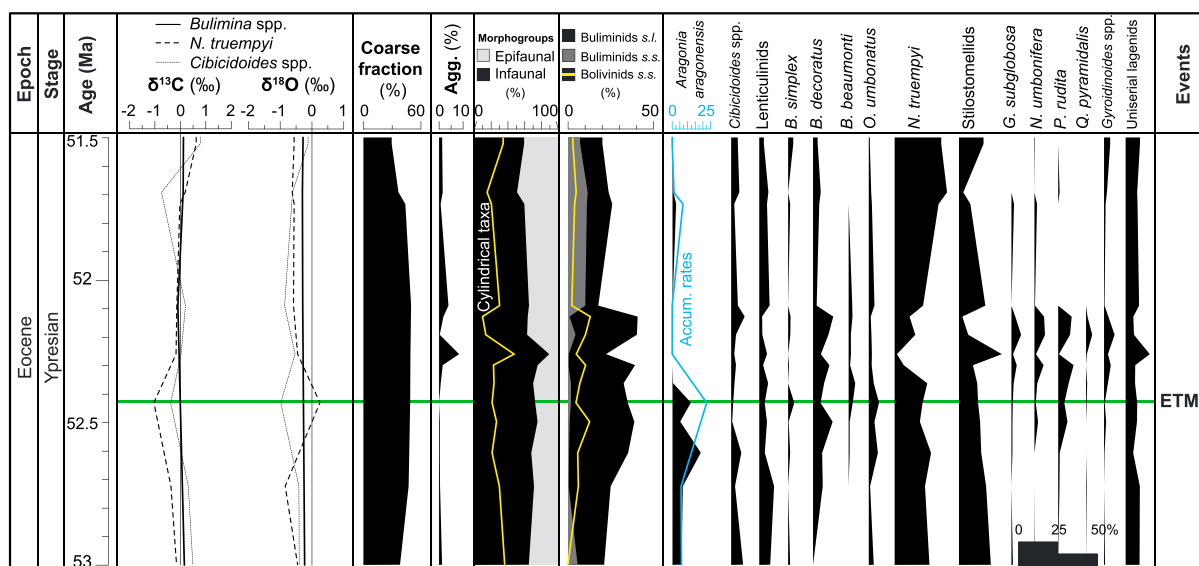


Figure 6. $\delta^{13}\text{C}$ and $\delta^{18}\text{O}$ values in benthic foraminiferal species across ETM3 event at ODP Site 865. Percentages of agglutinated taxa, infaunal-epifaunal morphogroups, cylindrical taxa, buliminids s.l., buliminids s.s., and bolivinids s.s. Relative abundance of selected benthic foraminiferal taxa and percentage of coarse fraction. Stable isotope data from *Bralower et al.* [1995a, 1995b] and *Katz et al.* [2003].

The MECO event at ~40 Ma [Bohatty et al., 2009; Westerhold and Röhl, 2013] was not recognized in the isotope record at the resolution of our studies. This age interval coincides with very low BFAR values at Site 865, immediately above the largest peak in BFAR. Benthic assemblages at ~40 Ma are characterized by a decrease in abundance of stilostomellids and *N. truempyi*, and by a slight increase in buliminids s.l., pleurostomellids, and uniserial lagenids (Figure S8 and Table S1).

5. Discussion

5.1. Coarse Fraction Weight Percent

At Site 865, the CF% is above 10% in almost all samples and above 25% in many samples (Figure 2). This is unusually high as compared to carbonate oozes at other drill sites, e.g., Walvis Ridge and Maud Rise [e.g., Kelly et al., 2010, 2012]. This high CF%, dominated by planktic foraminifera, probably reflects current winnowing on the seamount, which removed the fine (calcareous nannoplankton) fraction [e.g., Sager et al., 1993]. Changes in CF% thus can be seen as reflecting current activity across the top of Allison Guyot, with higher values indicating more winnowing. Increased winnowing occurred during warmer periods, with peak CF% across the PETM, a smaller peak across ETM3, and generally high values throughout the warm early Eocene, followed by a decline coeval with the high-latitude cooling starting in the early middle Eocene (Figures 2 and 4).

Such increased current activity during warm periods might appear surprising, because warm time periods have traditionally been seen as characterized by “sluggish ocean circulation” (e.g., Fischer and Arthur, 1977; see review in Thomas et al [2000]). In the planktic foraminifera, morozovellids and acarainids shift to deeper habitats, thus indicating that the water column structure changed during PETM warming [Kelly et al., 1996, 1998], as supported by climate modeling [Winguth et al., 2012]. Such changes in stratification may have influenced current patterns around the seamount [Lavelle and Mohn, 2010]. In addition, in Greenhouse climates such as that of the early Eocene sea surface temperatures are high, and intense hurricane activity drives a strong mixing in the upper tropical oceans [Korty et al., 2008]. Such increased hurricane activity during warm climates [e.g., Emanuel, 2002; Srivier and Huber, 2007] might have supplied temporary increased energy for enhanced current activity over seamounts, with deeper vertical mixing.

Alternatively, changes in deep water circulation [e.g., Thomas, 2004; Thomas et al., 2008; Hague et al., 2012] may have contributed to increased current activity at Site 865. For example, the mixing of deep waters sourced from the Southern Ocean, and the North Pacific in the tropical Pacific during the Paleogene

(~65 to ~45 Ma) [Thomas *et al.*, 2008], together with the steep topography of the Mid-Pacific mountain chain, may have influenced the hydrodynamics around the seamount.

The use of CF%, as a proxy for winnowing, points to a decrease in current activity during the early Lutetian (Figures 2 and 4). There is no evidence that surface waters in the tropical region of Site 865 cooled at that time [Pearson *et al.*, 2007], and stratification may have become more pronounced due to high-latitude (thus deep water) cooling, making deep mixing due to hurricane activity less pronounced. Alternatively, current patterns may have changed as the site was drifting northward from ~2°N (in the Paleocene) to 6°N (in the late Eocene) [Bralower *et al.*, 1995a], and the geographic extent of the zone of the highest hurricane activity may have changed [Kossin *et al.*, 2014].

5.2. Benthic Foraminifera

Benthic foraminiferal assemblages at Site 865 are highly diverse and heterogeneous, as expected for deep-sea faunas. The strong dominance by calcareous taxa throughout the studied interval is compatible with the location of this site at a paleodepth of 1300–1500 m, considerably above the CCD during most of the studied time interval [Pälike *et al.*, 2012]. The benthic foraminifera on Allison Guyot Site 865 generally represent cosmopolitan taxa [Thomas, 1998; Hayward *et al.*, 2012], and no endemic species were identified, supporting the observations on modern taxa of the importance of a motile life stage [Alve and Goldstein, 2003, 2010].

The dominance of long-term assemblages by infaunal taxa (mainly cylindrical taxa) throughout the studied interval, in an oligotrophic setting as inferred from planktic foraminifera [Kelly *et al.*, 1996, 1998] and calcareous nannofossils [Bralower *et al.*, 1995a] and at low overall BFAR values, appears unexpected, but we argue that this might reflect a seamount top ecosystem. Interpretation of species abundances is complex in seamount settings, where the selective advantage of morphotypes under an active current regime must be considered. Attached epifaunal taxa are abundant under such conditions [e.g., Schoenfeld, 2002], and detritivore infaunal taxa are generally rare because the sediment contains insufficient fine-grained organic matter to support deposit feeders [Heinz *et al.*, 2004]. However, both infaunally positioned suspension feeders anchored by spines and attached epifaunal suspension feeders may be common. We suggest that the spinose cylindrical taxa most common throughout the studied interval (stilostomellid species of the genus *Strictocostella*) [Hayward *et al.*, 2012] may have been shallow infaunally living species, according to their shape, distribution, and carbon isotope signature [Hayward and Kawagata, 2005; Hayward *et al.*, 2012; Mancin *et al.*, 2013], anchored in the sediment by their spines [Hottinger, 2000] and suspension feeding in the water column using their pseudopods extended through the complex aperture [e.g., Hottinger, 2000, 2006; Mancin *et al.*, 2013]. Such a lifestyle would be in agreement with suggestions that they were infaunal, k-strategist taxa with low metabolic rates [Mancin *et al.*, 2013], and rules out the possibility of reworking as the cause of their high numbers in the sediment. Consequently, we suggest that changes in the assemblages over time dominantly reflect changes in current activity (thus food supplied to the benthic foraminifera) rather than changes in primary productivity, even if planktic foraminifera and nannofossils suggest decreased productivity during the PETM [Kelly *et al.*, 1996, 1998]. Benthic foraminiferal assemblages do not show convincing evidence for a strong decline in oxygen availability.

Unfortunately, we cannot simply interpret the CF% data in terms of relative abundance of the spinose stilostomellids. Assemblages are easy to interpret only when one specific environmental factor dominates, e.g., food supply, but interaction between active currents and food transport (and, at times, changes in carbonate corrosivity) means that critical thresholds may play a role [Murray, 2001]. Higher current activity could result in lower food supply through more winnowing and removal of food particles or in increased food particles through trophic focusing.

In the late Paleocene, for instance, CF% increased slightly, while BFARs declined gradually as did the relative abundance of stilostomellids, while the oligotrophic indicator *N. truempyi* increased. The benthic foraminiferal data thus indicate decreasing food supply to the benthos in the latest part of the Paleocene, while current strength increased (Figure 7). During the earliest Eocene, however, and especially during the PETM the correlations were more complex (see below), and overall reversed, with higher cylindrical taxa% during high CF%. With the decline in CF% at about 47 Ma, however, we again see negative correlation with cylindrical taxa% (Figure 4). We argue that the situation during the PETM may reflect combined effects of increasing current strength and ocean acidification.

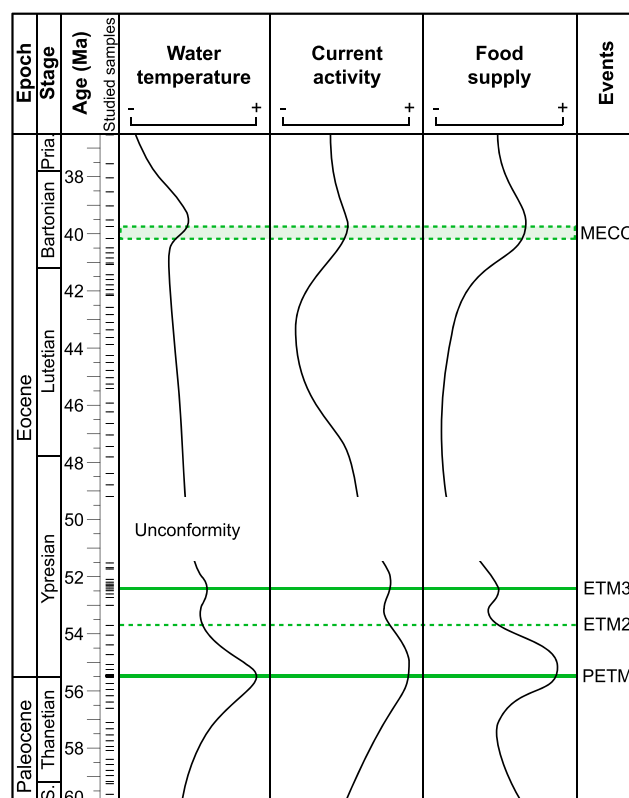


Figure 7. Long-term evolution of inferred environmental parameters across the upper Paleocene to middle Eocene at ODP Site 865.

The beginning of the PETM coincides with negative excursions in benthic foraminiferal $\delta^{13}\text{C}$ and $\delta^{18}\text{O}$ and CaCO_3 dissolution, followed by reprecipitation, as reflected in the occurrence of euhedral calcite crystals around foraminifera in the PETM interval and in that interval only (Figure S1) [Kozdon *et al.*, 2013]. The high $\%\text{CaCO}_3$ content despite dissolution is probably related to the lack of fine-grained terrestrial material in biogenic sediments deposited on the current-swept top of the guyot, so that CaCO_3 dissolution could not result in formation of a clay mineral layer. During carbonate dissolution, pore waters may become highly saturated in carbonate [Ilyina and Zeebe, 2012], so that infaunal benthic foraminifera are shielded from the corrosive waters [Foster *et al.*, 2013], whereas epifaunal taxa are exposed and may no longer be able to survive. High CF% values point to increased current activity (Figure 4).

At Site 865, as globally, large and heavily calcified taxa (e.g., *Stens. beccariiformis*) became extinct at the start of the PETM, and 33.4% (including local disappearances) of the species suffered extinction.

During the main phase of the CIE, the epifaunal *N. truempyi*, a survivor species of the extinction living exposed to bottom waters, was ecologically displaced, as at Antarctic Sites 689 and 690 [Thomas and Shackleton, 1996; Thomas, 2003]. We speculate that the smooth-walled taxa (buliminids and pleurostomellids) may have lived deeper in the sediment than the spinose suspension feeders, calcifying in less carbonate-undersaturated pore waters, as did trochospiral infaunal species *Oridorsalis umbonatus* at Walvis Ridge sites [Foster *et al.*, 2013]. In the Wagner Basin (Gulf of California, Mexico), buliminids are abundant without signs of dissolution under corrosive conditions close to carbon dioxide-emitting vents [Hart *et al.*, 2012]. These deeper infaunal taxa thus could have become dominant (up to 96% of the assemblages) even at high current activity (maximum CF%, Figures 2 and 3) and in the absence of a higher food supply, through lack of competition of epifaunal and shallow infaunal species which could not survive in the CaCO_3 corrosive waters. However, possibly, more food may have become available to infaunal deposit feeders even at declining primary productivity [Kelly *et al.*, 1996; Winguth *et al.*, 2012], because changing current conditions might have led to trophic focusing at the location of Site 865, thus enhanced BFAR values and higher percentages of buliminids and pleurostomellids. The scarcity of ostracodes, organisms without a motile life stage [Yamaguchi and Norris, 2015], might have been caused not by a decline in food but by carbonate corrosiveness and the high current regime, followed by lack of reimmigration.

High relative abundances of small, thin-walled abyssamminid species directly after the benthic extinction have been documented at many sites [Thomas, 1998], e.g., on Pacific Shatsky Rise Sites 1209–1211 [Takeda and Kaiho, 2007], on Southeast Atlantic Walvis Ridge Sites 525 and 527 [Thomas and Shackleton, 1996], and the western Tethys [Alegret *et al.*, 2009a], but these species are absent during the PETM at Site 865 (Figure 3). We suggest that these small species may have not been able to thrive under the current conditions on the seamount, or the food supply may have been too high for these abyssal species adapted to very oligotrophic conditions.

At about 80 kyr after the beginning of the PETM, large and flat *Cibicidoides* with coarse pores on the spiral side increased in relative abundance, an unusual feature for PETM assemblages [Thomas, 1998]. Possibly, these species resembled the living *Cibicidoides wuellerstorfi* [Lutze and Thiel, 1989] or *Cibicidoides lobatulus* [Dubicka et al., 2015; Gooday et al., 2015], living epifaunally attached to hard surfaces [Thomas, 1998]. These epifaunal species could not thrive during the phase of deep-sea ocean acidification during peak PETM, but they may have become abundant when currents were still too strong to allow reestablishment of the shallow infaunal suspension feeders [Schoenfeld, 2002] and corrosiveness declined. We do not know whether the *Cibicidoides* were currently distributed from outcropping rock surface to the edge of the guyot or lived attached to sessile animals close to the location of Site 865. Subsequently, the percentage of *Cibicidoides* spp. gradually decreased, probably due to less transport of shells or due to decreased food supply associated with declining current strength. After the dissolution interval of the PETM, CF% (thus possibly current strength) declined, the abundance of buliminids s.l. (including the opportunistic species *T. selmensis*) decreased and the abundance of the cylindrical and spinose stilostomellids (including *S. pseudoscripta*) increased again.

No evidence for significant dissolution (euhedral calcite crystals) has been observed across the ETM3 at Site 865. A moderate increase in food supply to the seafloor is inferred from increased BFAR values and percentage of buliminids s.l. (Figures 2 and 7). The species *P. rudita* shows greatest abundances at intermediate paleodepths [Tjalsma and Lohmann, 1983]; hence, its increase in abundance after the ETM3 may be related to an increased food availability, which allowed this species to thrive at somewhat greater paleodepths, such as at Site 865. The species *A. aragonensis* is a potentially opportunistic species [Steineck and Thomas, 1996], which has been interpreted as a marker of hyperthermal events due to its proliferation during and after Paleogene warming events [Thomas, 1990, 1998, 2003; Alegret et al., 2009a, 2009b; Giusberti et al., 2009; Ortiz et al., 2011]. The species peaked in abundance after the PETM [Thomas, 1998] and during the ETM3 at Site 865, supporting the interpretation of this species as a marker of early Eocene hyperthermal events. This species may have proliferated during warm intervals but not under carbonate corrosive conditions, which would explain why its abundance peak occurred after the peak PETM.

In the upper half of the studied interval (~51.5–36.5 Ma; after ETM3 then following the unconformity), a moderate increase in the food supply to the benthos is inferred from the gradual decrease in relative abundance of *N. truempyi* and higher percentages of buliminids s.s. and cylindrical taxa (Figure 2), with lower CF% once again associated with other benthic indicators of somewhat higher food supply, as in the late Paleocene. A slight increase is recorded from 43 to 40 Ma, possibly related to more intense winnowing by currents toward the MECO.

We thus interpret the late Paleocene-middle Eocene benthic assemblages on a Pacific seamount during a warming-cooling long-term evolution punctuated by short hyperthermal events as follows:

1. The dominance of infaunal, cylindrical taxa with complex apertures reflects the ecological success of these shallowly infaunal dwelling suspension feeders in the current-swept environment of the guyot top. This group was, however, less successful under the CaCO₃ corrosive conditions of the PETM, and declined in abundance (Figure 5), with spinose stilostomellids being replaced by smooth-walled pleurostomellids (Figure S8).
2. Buliminids s.l. increase in relative abundance in intervals with increased CF% and decreased percentages of *N. truempyi*, an oligotrophic species (Figure 5). The increased relative abundance of buliminids s.l. may have been due to increased food supply because of trophic focusing during the PETM or around the MECO interval, independent of primary productivity. Alternatively, this group may have proliferated under CaCO₃ corrosive conditions, as their deeper infaunal lifestyle in less undersaturated pore waters may have protected them (e.g., during the PETM) [Foster et al., 2013].
3. The infaunal cylindrical taxa may have lived closer to the sediment-water interface because of their suspension-feeding lifestyle than the deposit-feeding buliminids and thus were less sheltered from dissolution. Lenticulinids, another dissolution-resistant group with an infaunal lifestyle, did not peak in abundance at Site 865, probably as a consequence of their different feeding strategies and lack of ecological success where suspension feeders thrive.
4. The highest percentage of coarse fraction occurred during the recovery period of the PETM and overlaps with high relative abundances of *Cibicidoides* spp. (Figure 5), reflecting the adaptation of these species to high current conditions attached to hard surfaces [Thomas, 1998], but they live epifaunally and have coarse pores and thus are susceptible to dissolution and cannot thrive under CaCO₃ corrosive conditions.

5. The distribution pattern of *N. truempyi*, which in the upper Paleocene is negatively correlated to BFAR and positively correlated to CF%, is interpreted as indicative of oligotrophic conditions. The high abundances of this species during the early-middle Eocene (53.7 to ~44 Ma) were also correlated to intervals with higher CF% and lower percentage of cylindrical taxa, thus more oligotrophic conditions. Its disappearance during the PETM may reflect the occurrence of combined CaCO₃ corrosive waters, a high current regime, and/or ecological competition with taxa benefited from increased food availability. The species is generally common during warm conditions [e.g., Takeda and Kaiho, 2007; Alegret et al., 2009a, 2009b; Giusberti et al., 2009; Boscolo-Galazzo et al., 2013], and at Site 865 its abundance declined toward the upper part of the middle Eocene, coinciding with progressive cooling of sea bottom waters as inferred from higher benthic $\delta^{18}\text{O}$ values (Figure 2).

In spite of the unusual conditions on a seamount setting, the extinction of benthic foraminifera at the start of the PETM is comparable to that at other sites where more than 30% of the species went extinct or temporarily disappeared [e.g., Thomas, 1990; Thomas and Shackleton, 1996; Takeda and Kaiho, 2007; Alegret et al., 2009a, 2009b]. The geographic isolation of the seamount thus does not seem to have affected the extinction and recovery of the assemblages after the PETM, in contrast with ostracodes, which show more severe extinction and a much longer recovery period at Allison Guyot [Yamaguchi and Norris, 2015] than in the North Atlantic [Yamaguchi and Norris, 2012] and the Southern Ocean [Steineck and Thomas, 1996; Webb et al., 2009]. This differential response in ostracodes to the PETM probably results from the fact that benthic ostracodes are not efficient in dispersal [Yasuhara et al., 2012; Yamaguchi and Norris, 2015], whereas benthic foraminifera are highly efficient [Alve and Goldstein, 2003, 2010].

6. Conclusions

Pelagic sediments deposited on the flat top of Allison Guyot (Mid-Pacific Mountains) at equatorial Pacific ODP Site 865 provide a long-term record of benthic foraminifera across the late Paleocene-middle Eocene and allow us to reconstruct the faunal and paleoenvironmental turnover in an unusual, isolated, and current-swept seamount setting. The late Paleocene was characterized by a progressive increase in current activity and oligotrophic conditions, but the food input to the bottom-dwelling fauna suddenly increased at the Paleocene-Eocene boundary, even under declining primary productivity. These conditions of high current activity and food supply persisted until ~54 Ma. Afterward, the food supply became more moderate, and oligotrophic taxa like *N. truempyi* started to dominate the assemblages up to the middle Eocene (~43 Ma). Current activity gradually increased (~42 Ma) after a drop at the middle Eocene (~47 Ma) and remained relatively high up to the Priabonian, although it did not reach the high activity recorded during the late Paleocene-early Eocene.

Assemblage changes across the PETM and ETM3 were similar, with both events possibly associated with increased food supply through trophic focusing. Faunas across the PETM may have been affected by a combination of carbonate corrosion and locally increased food supply through trophic focusing due to enhanced current activity, followed by increased current activity after recovery from carbonate dissolution. During the ETM3, assemblages were affected by trophic focusing but not by severe dissolution.

The benthic foraminiferal turnover at Allison Guyot was controlled by a combination of long-term global change and superimposed short-term hyperthermal events, through changes in local current systems around the guyot top rather than changes in primary productivity or organic remineralization.

References

- Agnini, C., P. Macri, J. Backman, H. Brinkhuis, E. Fornaciari, L. Giusberti, V. Luciani, D. Rio, A. Sluijs, and F. Speranza (2009), An early Eocene carbon cycle perturbation at ~52.5 Ma in the Southern Alps: Chronology and biotic response, *Paleoceanography*, 24, PA2209, doi:10.1029/2008PA001649.
- Alegret, L., and E. Thomas (2001), Upper Cretaceous and lower Paleogene benthic foraminifera from northeastern Mexico, *Micropaleontology*, 47(4), 269–316.
- Alegret, L., and E. Thomas (2005), Cretaceous/Paleogene boundary bathyal paleo-environments in the central North Pacific (DSDP Site 465), the Northwestern Atlantic (ODP Site 1049), the Gulf of Mexico and the Tethys: The benthic foraminiferal record, *Palaeogeogr. Palaeoecol.*, 224, 53–82, doi:10.1016/j.palaeo.2005.03.031.
- Alegret, L., and E. Thomas (2009), Food supply to the seafloor in the Pacific Ocean after the Cretaceous Paleogene boundary event, *Mar. Micropaleontol.*, 73, 105–116, doi:10.1016/j.marmicro.2009.07.005.
- Alegret, L., S. Ortiz, and E. Molina (2009a), Extinction and recovery of benthic foraminifera across the Paleocene-Eocene thermal maximum at the Alamedilla section (Southern Spain), *Palaeogeogr. Palaeoclimatol. Palaeoecol.*, 279, 186–200.

Acknowledgments

This paper benefitted from comments of three anonymous reviewers. G.J.A.R. and L.A. acknowledge funding from project CGL2014-58794-P (Spanish Ministry of Economy and Competitiveness and FEDER funds) and Consolidated Group E05 (Government of Aragon/European Social Fund) and E. T. from NSF OCE-720049 and the Leverhulme Trust. G.J.A.R. thanks the Consejo Nacional de Ciencia y Tecnología (Conacyt, México) for her predoctoral fellowship. This research used samples provided by the Ocean Drilling Program (ODP), sponsored by the U.S. National Science Foundation (NSF) and participating countries under management of Joint Oceanographic Institutions (JOI), Inc., and is part of the PhD thesis of the first author. All the data employed in this paper are available in the supporting information (Tables S1–S5) and may also be requested from Gabriela Arreguín-Rodríguez (arreguin@unizar.es) or Laia Alegret (laia@unizar.es).

- Alegret, L., S. Ortiz, X. Orue-Etxebarria, G. Bernaola, J. I. Baceta, S. Monechi, E. Apellaniz, and V. Pujalte (2009b), The Paleocene-Eocene thermal maximum: New data on microfossil turnover at the Zumaia section, Spain, *Palaiois*, **24**, 318–328.
- Alegret, L., S. Ortiz, I. Arenillas, and E. Molina (2010), What happens when the ocean is overheated? The foraminiferal response across the Paleocene–Eocene thermal maximum at the Alamedilla section (Spain), *GSA Bull.*, **122**(9/10), 1616–1624.
- Alve, E., and S. T. Goldstein (2003), Propagule transport as a key method of dispersal in benthic foraminifera (Protista), *Limnol. Oceanogr.*, **48**, 2163–2170.
- Alve, E., and S. T. Goldstein (2010), Dispersal, survival and delayed growth of benthic foraminiferal propagules, *J. Sea Res.*, **63**, 36–51.
- Bohaty, S. M., and J. C. Zachos (2003), Significant Southern Ocean warming event in the late middle Eocene, *Geology*, **31**(11), 1017–1020.
- Bohaty, S. M., J. C. Zachos, F. Florindo, and M. L. Delaney (2009), Coupled greenhouse warming and deep-sea acidification in the middle Eocene, *Paleoceanography*, **24**, PA2207, doi:10.1029/2008PA001676.
- Boomer, I., and R. Whatley (1995), Cenozoic Ostracoda from guyots in the western Pacific: Holes 865B and 866B (Leg 143), in *Proceedings of the Ocean Drilling Program, Sci. Results*, vol. 143, edited by E. L. Winterer et al., pp. 75–86, Ocean Drill. Program, College Station, Tex.
- Boscolo-Galazzo, F., L. Giusberti, V. Luciani, and E. Thomas (2013), Paleoenvironmental changes during the Middle Eocene Climatic Optimum (MECO) and its aftermath: The benthic foraminiferal record from the Alano section (NE Italy), *Palaeogeogr. Palaeoclimatol. Palaeoecol.*, **378**, 22–35.
- Boscolo-Galazzo, F., E. Thomas, M. Pagani, C. Warren, V. Luciani, and L. Giusberti (2014), The middle Eocene climatic optimum (MECO): A multi-proxy record of paleoceanographic changes in the southeast Atlantic (ODP Site 1263, Walvis Ridge), *Paleoceanography*, **29**, 1143–1161, doi:10.1002/2014PA002670.
- Boyd, P. W., and T. W. Trull (2007), Understanding the export of biogenic particles in oceanic waters: Is there consensus?, *Prog. Oceanogr.*, **72**, 276–312.
- Bralower, T. J., and J. Mutterlose (1995), Calcareous nannofossil biostratigraphy of Site 865, Allison Guyot, central Pacific Ocean: A tropical Paleogene reference section, in *Proceedings of the Ocean Drilling Program, Sci. Results*, vol. 143, edited by E. L. Winterer et al., pp. 31–74, Ocean Drill. Program, College Station, Tex.
- Bralower, T. J., J. C. Zachos, E. Thomas, M. Parrow, C. K. Paul, D. C. Kelly, I. Premoli Silva, W. V. Sliter, and K. C. Lohmann (1995a), Late Paleocene to Eocene paleoceanography of the equatorial Pacific Ocean: Stable isotopes recorded at Ocean Drilling Program Site 865, Allison Guyot, *Paleoceanography*, **10**, 841–865, doi:10.1029/95PA01143.
- Bralower, T. J., M. Parrow, E. Thomas, and J. C. Zachos (1995b), Data report: Stable isotope stratigraphy of the Paleogene pelagic cap at Site 865, Allison Guyot, in *Proceedings of the Ocean Drilling Program, Sci. Results*, vol. 143, edited by E. L. Winterer et al., pp. 581–586, Ocean Drill. Program, College Station, Tex.
- Burkett, A. M., A. E. Rathburn, M. E. Perez, L. A. Levin, H. Cha, and G. W. Rouse (2015), Phylogenetic placement of *Cibicidoides wuellerstorfi* (Swager, 1866) from methane seeps and non-seep habitats on the Pacific margin, *Geobiology*, **13**, 44–52.
- Buzas, M. A., S. J. Culver, and F. J. Jorissen (1993), A statistical evaluation of the microhabitats of living (stained) infaunal benthic foraminifera, *Mar. Micropaleontol.*, **20**, 311–320.
- Chun, C. O. J., M. L. Delaney, and J. C. Zachos (2010), Paleoredox changes across the Paleocene-Eocene thermal maximum, Walvis Ridge (ODP Sites 1262, 1263, and 1266): Evidence from Mn and U enrichment factors, *Paleoceanography*, **25**, PA4202, doi:10.1029/2009PA001861.
- Colosimo, A. B., T. J. Bralower, and J. C. Zachos (2005), Evidence for lysocline shoaling and methane hydrate dissociation at the Paleocene-Eocene thermal maximum on Shatsky Rise, in *Proceedings of the Ocean Drilling Program, Sci. Results*, vol. 198, edited by T. J. Bralower, I. Premoli Silva, and M. J. Malone, 36 pp., Texas A&M Univ., College Station, Tex.
- Cramer, B. S., J. D. Wright, D. V. Kent, and M. Aubry (2003), Orbital climate forcing of the $\delta^{13}\text{C}$ excursions in the late Paleocene-early Eocene (chrons C24n–C25n), *Paleoceanography*, **18**(4), 1097, doi:10.1029/2003PA000909.
- de Conto, R. M., S. Galeotti, M. Pagani, D. Tracy, K. Schaefer, T. Zhang, D. Pollard, and D. J. Beerling (2012), Past extreme warming events linked to massive carbon release from thawing permafrost, *Nature*, **484**, 87–91.
- de Forges, B. R., J. A. Koslow, and G. C. B. Poore (2000), Diversity and endemism of the benthic seamount fauna in the southwest Pacific, *Nature*, **405**, 944–947.
- d’Haenens, S., A. Bornemann, P. Stassen, and R. Speijer (2012), Multiple early Eocene benthic foraminiferal assemblages and $\delta^{13}\text{C}$ fluctuations at DSDP Site 401 (Bay of Biscay—NE Atlantic), *Mar. Micropaleontol.*, **88–89**, 15–35.
- Dickens, G. R. (2011), Down the rabbit hole: Toward appropriate discussion of methane release from gas hydrate systems during the Paleocene–Eocene thermal maximum and other past hyperthermal events, *Clim. Past*, **7**(3), 831–846.
- Dickens, G. R., J. R. O’Neil, D. K. Rea, and R. M. Owen (1995), Dissociation of oceanic methane hydrate as a cause of the carbon isotope excursion at the end of the Paleocene, *Paleoceanography*, **10**, 965–971, doi:10.1029/95PA02087.
- Dickens, G. R., M. M. Castillo, and J. C. G. Walker (1997), A blast of gas in the latest Paleocene: Simulating first-order effects of massive dissociation of oceanic methane hydrate, *Geology*, **25**(3), 259–262.
- Dower, J. F., and R. D. Brodeur (2004), The role of biophysical coupling in concentrating marine organisms around shallow topographies, *J. Mar. Sci.*, **50**, 1–2.
- Dubicka, Z., M. Zlotnik, and T. Borszcz (2015), Test morphology as a function of behavioral strategies—Inferences from benthic foraminifera, *Mar. Micropaleontol.*, **116**, 38–49.
- Dunkley Jones, T., D. J. Lunt, D. N. Schmidt, A. Ridgwell, A. Sluijs, P. J. Valdes, and M. A. Maslin (2013), Climate model and proxy data constraints on ocean warming across the Paleocene-Eocene thermal maximum, *Earth Sci. Rev.*, **125**, 123–145.
- Edgar, K. M., P. A. Wilson, P. F. Sexton, and Y. Suganuma (2007), No extreme bipolar glaciation during the main Eocene calcite compensation shift, *Nature*, **448**, 908–911.
- Edgar, K. M., E. Anagnostou, P. N. Pearson, and G. L. Foster (2015), Assessing the impact of diagenesis on $\delta^{11}\text{B}$, $\delta^{13}\text{C}$, $\delta^{18}\text{O}$, Sr/Ca and B/Ca values in fossil planktic foraminiferal carbonate, *Geochim. Cosmochim. Acta*, **166**, 189–209.
- Eldrett, J. S., D. R. Greenwood, M. Polling, H. Brinkhuis, and A. Sluijs (2014), A seasonality trigger for carbon injection at the Paleocene Eocene thermal maximum, *Clim. Past*, **10**, 759–769.
- Emanuel, K. (2002), A simple model of multiple climate regimes, *J. Geophys. Res.*, **107**(D9), 4077, doi:10.1029/2001JD001002.
- Fischer, A. G., and M. A. Arthur (1977), Secular variations in the pelagic realm, *SEPM Spec. Publ.*, **25**, 19–150.
- Fontanier, C., F. J. Jorissen, L. Licari, A. Alexandre, P. Anschutz, and P. Carbonel (2002), Live benthic foraminiferal faunas from the Bay of Biscay: Faunal density, composition, and microhabitats, *Deep Sea Res., Part I*, **49**, 751–785.
- Foster, L. C., D. N. Schmidt, E. Thomas, S. Arndt, and A. Ridgwell (2013), Surviving rapid climate change in the deep sea during the Paleogene hyperthermals, *Proc. Natl. Acad. Sci. U.S.A.*, **110**(23), 9273–9276, doi:10.1073/pnas.1300579110.
- Galeotti, S., S. Krishnan, M. Pagani, L. Lanci, A. Gaudio, J. C. Zachos, S. Monechi, G. Morelli, and L. Lourens (2010), Orbital chronology of Early Eocene hyperthermals from the Contessa Road section, central Italy, *Earth Planet. Sci. Lett.*, **290**, 192–200.

- García-Muñoz, M., N. López-González, J. L. Rueda, D. Palomino, J. T. Vázquez, V. Díaz-del-Río, and M. C. Fernández-Puga (2012), Caracterización ambiental de montes submarinos del Mar de Alborán a partir del estudio de los sedimentos y las asociaciones de foraminíferos bentónicos, *Geogaceta*, 52, 165–168.
- Genin, A. (2004), Bio-physical coupling in the formation of zooplankton and fish aggregations over abrupt topographies, *J. Mar. Syst.*, 50, 3–20.
- Genin, A., P. K. Dayton, P. F. Lonsdale, and F. N. Spiess (1998), Corals on seamount peaks provide evidence of current acceleration over deep-sea topography, *Nature*, 322, 59–61.
- Giusberti, L., R. Coccioni, M. Sprovieri, and F. Tateo (2009), Perturbation at the sea floor during the Paleocene-Eocene thermal maximum: Evidence from benthic foraminifera at Contessa Road, Italy, *Mar. Micropaleontol.*, 70, 102–119.
- Gooday, A. J. (2003), Benthic foraminifera (Protista) as tools in deep-water palaeoceanography: Environmental influences on faunal characteristics, *Adv. Mar. Biol.*, 46, 1–90.
- Gooday, A. J., A. Goineua, and I. Voltski (2015), Abyssal foraminifera attached to polymetallic nodules from the eastern Clarion Clipperton Fracture Zone: A preliminary description and comparison with North Atlantic dropstone assemblages, *Mar. Biodiversity*, doi:10.1007/s12526-014-0301-9.
- Hague, A. M., D. J. Thomas, M. Huber, R. Korte, S. C. Woodard, and L. B. Jones (2012), Convection of North Pacific deep water during the early Cenozoic, *Geology*, 40(6), 527–530.
- Hammer, O., and D. A. T. Harper (2006), *Paleontological Data Analysis*, 351 pp., Blackwell, Mass.
- Handley, L., P. N. Pearson, I. K. McMillan, and R. D. Pancost (2008), Large terrestrial and marine carbon and hydrogen isotope excursions in a new Paleocene/Eocene boundary section from Tanzania, *Earth Planet. Sci. Lett.*, 275, 17–25.
- Hart, M., L. Pettit, D. Wall-Palmer, C. Smart, J. Hall-Spencer, A. Medina-Sanchez, R. M. Prol Ledesma, R. Rodolfo-Metalpa, and P. Collins (2012), Investigation of the calcification response of foraminifera and pteropods to high CO₂ environments in the Pleistocene, Paleogene and Cretaceous, paper presented at European Geosciences Union General Assembly 2012, Vienna, Austria.
- Hay, W., et al. (1999), Alternative global Cretaceous paleogeography, in *Evolution of the Cretaceous Ocean-Climate System, Spec. Pap.*, vol. 332, edited by E. Barrera and C. C. Johnson, pp. 1–47, Geol. Soc. of Am, Boulder, Colo.
- Hayward, B. W., and S. Kawagata (2005), Extinct foraminifera figured in Brady's challenger report, *J. Micropaleontol.*, 26, 171–175.
- Hayward, B. W., S. Kawata, A. Sabaa, H. Grenfell, L. van Kerckhoven, K. Johnson, and E. Thomas (2012), The last global extinction (mid-Pleistocene) of deep-sea benthic foraminifera (Chrysalogoniidae, Ellipsoidinidae, Glandulonodosariidae, Plectofrondiculariidae, Pleurostomellidae, Stilostomellidae), their late Cretaceous-Cenozoic history and taxonomy, *Cushman Found. Foraminiferal Res. Spec. Publ.*, 43, 408 pp.
- Heinz, P., D. Ruepp, and C. Hemleben (2004), Benthic foraminifera assemblages at Great Meteor Seamount, *Mar. Biol.*, 144, 985–998.
- Henson, S., R. Sanders, and E. Masden (2012), Global patterns in efficiency of particulate organic carbon export and transfer to the deep ocean, *Global Biogeochem. Cycles*, 26, GB1028, doi:10.1029/2011GB004099.
- Herguera, J. C., and W. H. Berger (1991), Paleoproductivity from benthic foraminifera abundance: Glacial to postglacial change in the west-equatorial Pacific, *Geology*, 19, 1173–1176.
- Higgins, J. A., and D. P. Schrag (2006), Beyond methane: Towards a theory for the Paleocene-Eocene thermal maximum, *Earth Planet. Sci. Lett.*, 245, 523–537.
- Hottinger, L. C. (2000), Functional morphology of benthic foraminiferal shells, envelopes of cells beyond measure, *Micropaleontology*, 46(1), 57–86.
- Hottinger, L. C. (2006), The "face" of benthic foraminifera, *Boll. Soc. Paleontol. Ital.*, 45, 75–89.
- Ilyina, T., and R. E. Zeebe (2012), Detection and projection of carbonate dissolution in the water column and deep-sea sediments due to ocean acidification, *Geophys. Res. Lett.*, 39, L06606, doi:10.1029/2012GL051272.
- Jennions, S. M., E. Thomas, D. N. Schmidt, D. J. Lunt, and A. Ridgwell (2015), Changes in benthic ecosystems and ocean circulation in the Southeast Atlantic across Eocene thermal maximum 2, *Paleoceanography*, 30, 1059–1077, doi:10.1002/2015PA002821.
- John, E. H., P. N. Pearson, H. K. Coxall, H. Birch, B. S. Wade, and G. L. Foster (2013), Warm ocean processes and carbon cycling in the Eocene, *Philos. Trans. R. Soc. A*, 371, doi:10.1098/rsta.2013.0099.
- John, E. H., J. D. Wilson, P. N. Pearson, and A. Ridgwell (2014), Temperature-dependent remineralization and carbon cycling in the warm Eocene oceans, *Palaeogeogr. Palaeoclimatol. Palaeoecol.*, 413, 158–166.
- Jorissen, F. J. (1999), Benthic foraminiferal successions across Late Quaternary Mediterranean sapropels, *Mar. Geol.*, 153, 91–101.
- Jorissen, F. J., H. C. Stigter, and J. G. V. Widmark (1995), A conceptual model explaining benthic foraminiferal microhabitats, *Mar. Micropaleontol.*, 26, 3–15.
- Jorissen, F. J., C. Fontanier, and E. Thomas (2007), Paleoceanographical proxies based on deep-sea benthic foraminiferal assemblages characteristics, in *Proxies in Late Cenozoic Paleoceanography: Part 2—Biological Tracers and Biomarkers*, edited by C. Hillaire-Marcel and A. Vernal, pp. 263–326, Elsevier, Amsterdam.
- Katz, M. E., D. R. Katz, J. D. Wright, K. G. Miller, D. K. Pak, N. J. Shackleton, and E. Thomas (2003), Early Cenozoic benthic foraminiferal isotopes: Species reliability and interspecies correction factors, *Paleoceanography*, 18(2), 1024, doi:10.1029/2002PA000798.
- Kelly, D. C., T. J. Bralower, J. C. Zachos, I. Premoli-Silva, and E. Thomas (1996), Rapid diversification of planktonic foraminifera in the tropical Pacific (ODP Site 865) during the late Paleocene thermal maximum, *Geology*, 24, 423–426.
- Kelly, D. C., T. J. Bralower, and J. C. Zachos (1998), Evolutionary consequences of the latest Paleocene thermal maximum for tropical planktonic foraminifera, *Palaeogeogr. Palaeoclimatol. Palaeoecol.*, 141, 139–161.
- Kelly, D. C., T. M. J. Nielsen, H. K. McCarren, J. C. Zachos, and U. Röhl (2010), Spatiotemporal patterns of carbonate sedimentation in the South Atlantic: Implications for carbon cycling during the Paleocene–Eocene thermal maximum, *Palaeogeogr. Palaeoclimatol. Palaeoecol.*, 293(1–2), 30–40.
- Kelly, D. C., T. M. J. Nielsen, and S. A. Schellenberg (2012), Carbonate saturation dynamics during the Paleocene–Eocene thermal maximum: Bathyal constraints from ODP sites 689 and 690 in the Weddell Sea (South Atlantic), *Mar. Geol.*, 303–306, 75–86.
- Kennett, J. P., and L. D. Stott (1991), Abrupt deep-sea warming, palaeoceanographic changes and benthic extinctions at the end of the Paleocene, *Nature*, 353, 225–229.
- Kirtland-Turner, S., and A. Ridgwell (2014), Recovering the true size of an Eocene hyperthermal from the marine sedimentary record, *Paleoceanography*, 28, 700–712, doi:10.1002/2013PA002541.
- Korte, R. L., K. A. Emanuel, and J. R. Scott (2008), Tropical cyclone-induced upper-ocean mixing and climate: Application to equable climates, *J. Clim.*, 21, 638–654.
- Kossin, J. P., K. A. Emanuel, and G. A. Vecchi (2014), The poleward migration of the location of tropical cyclone maximum intensity, *Nature*, 509, 349–352.
- Kozdon, R., D. C. Kelly, N. T. Kita, J. H. Fournelle, and J. W. Valley (2011), Planktonic foraminiferal oxygen isotope analysis by ion microprobe technique suggests warm tropical sea surface temperatures during the Early Paleogene, *Paleoceanography*, 26, PA3206, doi:10.1029/2010PA002056.

- Kozdon, R., D. C. Kelly, K. Kitajima, A. Strickland, J. H. Fournelle, and J. W. Valley (2013), In situ $\delta^{18}\text{O}$ and Mg/Ca analyses of diagenetic and planktic foraminiferal calcite preserved in a deep-sea record of the Paleocene-Eocene thermal maximum, *Paleoceanography*, 28, 517–528, doi:10.1002/palo.20048.
- Kurtz, A. C., L. R. Kump, M. A. Arthur, J. C. Zachos, and A. Paytan (2003), Early Cenozoic decoupling of the global carbon and sulfur cycles, *Paleoceanography*, 18(4), 1090, doi:10.1029/2003PA000908.
- Kustanowich, S. (1962), A foraminiferal fauna from Capricorn Seamount, southwest equatorial Pacific, *N. Z. J. Geol. Geophys.*, 5(3), 427–434.
- Lauretano, V., K. Littler, M. Polling, J. C. Zachos, and L. J. Lourens (2015), Frequency, magnitude and character of hyperthermia: Events at the onset of the early Eocene climatic optimum, *Clim. Past Discuss.*, 11, 1795–1820.
- Lavelle, W., and C. Mohn (2010), Motion, commotion, and biophysical connections at deep ocean seamounts, *Oceanography*, 23(1), 91–103.
- Leon-Rodriguez, L., and G. R. Dickens (2010), Constraints on ocean acidification associated with rapid and massive carbon injections: The early Paleogene record at ocean drilling program site 1215, equatorial Pacific Ocean, *Palaeogeogr. Palaeoclimatol. Palaeoecol.*, 298, 409–420.
- Littler, K., U. Röhl, T. Westerhold, and J. C. Zachos (2014), A high-resolution benthic stable-isotope record for the South Atlantic: Implications for orbital-scale changes in Late Paleocene–Early Eocene climate and carbon cycling, *Earth Planet. Sci. Lett.*, 401, 18–30.
- Loeblich, A. R., Jr., and H. Tappan (1987), *Foraminifera Genera and Their Classification*, Van Nostrand, New York.
- Lourens, L. J., A. Suijs, D. Kroon, J. C. Zachos, E. Thomas, U. Röhl, J. Bowles, and I. Raffi (2005), Astronomical pacing of late Palaeocene to early Eocene global warming events, *Nature*, 435, 1083–1087.
- Lunt, D. J., A. Ridgwell, A. Sluijs, J. C. Zachos, S. Hunter, and A. Haywood (2011), A model for orbital pacing of methane hydrate destabilization during the Paleogene, *Nat. Geosci.*, 4, 775–778.
- Lutze, G. F., and H. Thiel (1989), Epibenthic foraminifera from elevated microhabitats: *Cibicidoides wuellerstorfi* and *Planulina ariminensis*, *J. Foraminiferal Res.*, 19(2), 153–158.
- Ma, Z., E. Gray, E. Thomas, B. Murphy, J. C. Zachos, and A. Paytan (2014), Carbon sequestration during the Paleocene-Eocene thermal maximum by an efficient biological pump, *Nat. Geosci.*, 7, 382–388.
- Mackensen, A., G. Schmied, J. Harloff, and M. Giese (1995), Deep-sea foraminifera in the South Atlantic Ocean: Ecology and assemblage generation, *Micropaleontology*, 41, 342–358.
- Mancin, N., B. W. Hayward, I. Trattenero, M. Cobianchi, and C. Lupi (2013), Can the morphology of deep-sea benthic foraminifera reveal what caused their extinction during the mid-Pleistocene climate transition?, *Mar. Micropaleontol.*, 104, 53–70.
- Martin, J. H., G. A. Knauer, D. M. Karl, and W. W. Broenkow (1987), VERTEX: Carbon cycling in the north-east pacific, *Deep Sea Res.*, 34, 267–285.
- McCarren, H., E. Thomas, T. Hasegawa, U. Röhl, and J. C. Zachos (2008), Depth-dependency of the Paleocene-Eocene carbon isotope excursion: Paired benthic and terrestrial biomarker records (ODP Leg 208, Walvis Ridge), *Geochim. Geophys. Geosyst.*, 9, Q10008, doi:10.1029/2008GC002116.
- McClain, C. R. (2007), Seamounts: Identity crisis or split personality?, *J. Biogeogr.*, 34, 2001–2008.
- McClain, C. R., L. Lundsten, M. Ream, J. Barry, and A. DeVogelaere (2009), Endemicity, biogeography, composition and community structure on a Northwest Pacific Seamount, *PLoS One*, 4(1), e4141.
- McInerney, F. A., and S. Wing (2011), The Paleocene-Eocene thermal maximum: A perturbation of carbon cycle, climate, and biosphere with implications for the future, *Annu. Rev. Earth Planet. Sci.*, 39, 489–516.
- Mullineaux, L. S., and S. W. Mills (1997), A test of the larval retention hypothesis in seamount-generated flows, *Deep Sea Res., Part 1*, 44(5), 745–770.
- Murray, J. W. (2001), The niche of benthic foraminifera, critical thresholds and proxies, *Mar. Micropaleontol.*, 41, 1–7.
- Murray, J. (2006), *Ecology and Applications of the Benthic Foraminifera*, 426 pp., Cambridge Univ. Press, U. K.
- Nguyen, T. M. P., M. R. Petrizzo, and R. P. Speijer (2009), Experimental dissolution of a fossil foraminiferal assemblage (Paleocene-Eocene Thermal Maximum, Dababiya, Egypt): Implications for a paleoenvironmental reconstructions, *Mar. Micropaleontol.*, 73, 241–258, doi:10.1016/j.marmicro.2009.10.005.
- Nicolo, M. J., G. R. Dickens, C. J. Hollis, and J. C. Zachos (2007), Multiple early Eocene hyperthermals: Their sedimentary expression on the New Zealand continental margin and in the deep sea, *Geology*, 35(8), 699–702.
- Nienstedt, J., and A. J. Arnold (1988), The distribution of benthic foraminifera on seamounts near the East Pacific Rise, *J. Foraminiferal Res.*, 18(3), 237–249.
- Nisbet, E. G., S. M. Jones, J. Maclennan, G. Eagles, J. Moed, N. Warwick, S. Bekki, P. Braesicke, J. A. Pyle, and C. M. R. Fowler (2009), Kick-starting ancient global warming, *Nat. Geosci.*, 2, 156–159.
- Nunes, F., and R. D. Norris (2006), Abrupt reversal in ocean overturning during the Palaeocene/Eocene warm period, *Nature*, 439, 60–63.
- Ohkushi, K., and H. Natori (2001), Living benthic foraminifera of the Hess Rise and Suiko Seamount, central North Pacific, *Deep Sea Res., Part 1*, 48, 1309–1324.
- Ortiz, S., L. Alegret, A. Payros, X. Orue-Etxebarria, E. Apellaniz, and E. Molina (2011), Distribution patterns of benthic foraminifera across the Ypresian-Lutetian Gorrondatxe section, Northern Spain: Response to sedimentary disturbance, *Mar. Micropaleontol.*, 78, 1–13.
- Pagani, M., N. Pedentchouk, M. Huber, A. Sluijs, S. Schouten, H. Brinkhuis, J. S. Sinninghe Damsté, G. R. Dickens, and Expedition 302 Scientists (2006), Arctic hydrology during global warming at the Paleocene/Eocene thermal maximum, *Nature*, 442, 671–675.
- Pälike, C., M. L. Delaney, and J. C. Zachos (2014), Deep-sea redox across the Paleocene-Eocene thermal maximum, *Geochim. Geophys. Geosyst.*, 15, 1038–1053, doi:10.1002/2013GC005074.
- Pälike, H., et al. (2012), A Cenozoic record of the equatorial Pacific carbonate compensation depth, *Nature*, 488(7413), 609–614.
- Pawlowski, J., J. Fahrni, B. Lecroq, D. Longet, N. Cornelius, L. Escoffier, T. Cedhagen, and A. J. Gooday (2007), Bipolar gene flow in deep-sea benthic foraminifera, *Mol. Ecol.*, 16(19), 4089–4096.
- Payros, A., S. Ortiz, L. Alegret, X. Orue-Etxebarria, E. Apellaniz, and E. Molina (2012), An early Lutetian carbon-cycle perturbation: Insights from the Gorrondatxe section (western Pyrenees, Bay of Biscay), *Paleoceanography*, 27, PA2213, doi:10.1029/2012PA002300.
- Pearson, P. N., P. W. Ditchfield, J. Singano, K. G. Harcourt-Brown, C. J. Nicholas, R. K. Olsson, N. J. Shackleton, and M. A. Hall (2001), Warm tropical sea surface temperatures in the Late Cretaceous and Eocene epochs, *Nature*, 413, 481–487.
- Pearson, P. N., B. E. van Dongen, C. J. Nicholas, R. D. Pancost, S. Schouten, J. M. Singano, and B. S. Wade (2007), Stable warm tropical climate through the Eocene Epoch, *Geology*, 35, 211–214.
- Penman, D. E., B. Hoenisch, R. E. Zeebe, E. Thomas, and J. C. Zachos (2014), Rapid and sustained surface ocean acidification during the Paleocene-Eocene Thermal Maximum, *Paleoceanography*, 29, 357–369, doi:10.1002/2014PA002621.
- Röhl, U., T. Westerhold, S. Monechi, E. Thomas, J. C. Zachos, and B. Donner (2005), The third and final early Eocene thermal maximum: Characteristic, timing, and mechanisms of the “X” event, *Geol. Soc. Am. Abstr. Programs*, 37(7), 264.
- Sager, W. W., et al. (1993), Site 865, in *Proceedings of the Ocean Drilling Program, Initial Rep.*, vol. 143, edited by W. W. Sager et al., pp. 111–180, Ocean Drill. Program, College Station, Tex.

- Samadi, S., L. Bontan, E. Macpherson, B. R. de Forges, and M. C. Boisselier (2006), Seamount endemism questioned by the geographic distribution and population genetic structure of marine invertebrates, *Mar. Biol.*, **149**, 1463–1475.
- Schmiedl, G., A. Mitschele, S. Beck, K. C. Emeis, C. Hemleben, H. Schulz, M. Sperling, and S. Weldeab (2003), Benthic foraminiferal record of ecosystem variability in the eastern Mediterranean Sea during times of sapropel S₅ and S₆ deposition, *Palaeogeogr. Palaeoclimatol. Palaeoecol.*, **190**, 139–194.
- Schoenfeld, J. (2002), A new benthic foraminiferal proxy for near-bottom current velocities in the Gulf of Cadiz, northeastern Atlantic Ocean, *Deep Sea Res., Part I*, **49**, 1853–1875.
- Sen Gupta, B. K. (1999), Introduction to modern foraminifera, in *Systematics of Modern Foraminifera*, edited by B. K. Sen Gupta, pp. 7–36, Kluwer Acad., Dordrecht, Netherlands.
- Sen Gupta, B. K., and M. L. Machain-Castillo (1993), Benthic foraminifera in oxygen-poor habitats, *Mar. Micropaleontol.*, **20**, 3–4.
- Sexton, P. F., R. D. Norris, P. A. Wilson, H. Pälike, T. Westerhold, U. Röhl, C. T. Bolton, and S. Gibbs (2011), Eocene global warming events driven by ventilation of oceanic dissolved organic carbon, *Nature*, **471**, 349–352.
- Shank, T. M. (2010), Seamounts: Deep-ocean laboratories of faunal connectivity, evolution and endemism, *Oceanography*, **23**(1), 109–122.
- Sluijs, A., G. J. Bowen, H. Brinkhuis, L. J. Lourens, and E. Thomas (2007), The Paleocene-Eocene thermal maximum super greenhouse: Biotic and geochemical signatures, age models and mechanisms of global change, in *Deep time Perspectives on Climate Change: Marrying the Signal From Computer Models and Biological Proxies*, Spec. Publ., vol. 2, edited by M. Williams et al., pp. 323–349, Micropaleont. Soc. and Geol. Soc., London.
- Sluijs, A., S. Schouten, T. H. Donders, P. L. Schoon, U. Röhl, G. Reichert, F. Sangiorgi, J. Kim, J. S. Sinninghe Damsté, and H. Brinkhuis (2009), Warm and wet conditions in the Arctic region during Eocene thermal maximum 2, *Nat. Geosci.*, **2**, 777–780.
- Sluijs, A., R. E. Zeebe, P. K. Bijl, and S. M. Bohaty (2013), A middle Eocene carbon cycle conundrum, *Nat. Geosci.*, **6**(6), 429–434.
- Smart, C. W., E. Thomas, and A. T. S. Ramsay (2007), Middle-late Miocene benthic foraminifera in a western Indian Ocean depth transect: Paleoceneanographic implications, *Palaeogeogr. Palaeoclimatol. Palaeoecol.*, **247**, 402–420.
- Speijer, R. P., C. Scheibner, P. Stassen, and A. M. M. Morsi (2012), Response of marine ecosystems to deep-time global warming: A synthesis of biotic patterns across the Paleocene-Eocene thermal maximum (PETM), *Aust. J. Earth Sci.*, **105**, 6–16.
- Sriver, R. L., and M. Huber (2007), Observational evidence for an ocean heat pump induced by tropical cyclones, *Nature*, **447**, 577–580.
- Stap, L., A. Sluijs, E. Thomas, and L. Lourens (2009), Patterns and magnitude of deep sea carbonate dissolution during Eocene thermal maximum 2 and H2, Walvis Ridge, southeastern Atlantic Ocean, *Paleoceanography*, **24**, PA1211, doi:10.1029/2008PA001655.
- Stap, L., L. J. Lourens, E. Thomas, A. Sluijs, S. Bohaty, and J. C. Zachos (2010), High-resolution deep-sea carbon and oxygen isotope records of Eocene thermal maximum 2 and H2, *Geology*, **38**(7), 607–610.
- Staudigel, H., A. A. P. Koopers, W. J. Lavelle, T. J. Pitcher, and T. M. Shank (2010), Defining the word “seamount”, *Oceanography*, **23**(1), 20–21.
- Steineck, P. L., and E. Thomas (1996), The latest Paleocene crisis in the deep sea: Ostracode succession at Maud Rise, Southern Ocean, *Geology*, **24**, 583–586.
- Storey, M., R. A. Duncan, and C. C. Swisher Jr. (2007), Paleocene-Eocene thermal maximum and the opening of the Northeast Atlantic, *Science*, **316**, 587–589.
- Svensen, H., S. Planke, A. Malthes-Sørensen, B. Jamtveit, R. Myklebust, T. R. Eidem, and S. S. Rey (2004), Release of methane from a volcanic basin as a mechanism for initial Eocene global warming, *Nature*, **429**, 542–545.
- Svensen, H., S. Planke, and F. Corfu (2010), Zircon dating ties NE Atlantic sill emplacement to initial Eocene global warming, *J. Geol. Soc. London*, **167**, 433–436.
- Takeda, K., and K. Kaiho (2007), Faunal turnovers in central Pacific benthic foraminifera during the Paleocene-Eocene thermal maximum, *Palaeogeogr. Palaeoclimatol. Palaeoecol.*, **251**, 175–197.
- Thistle, D., and L. A. Levin (1998), The effect of experimentally increased near-bottom flow on metazoan meiofauna at a deep-sea site, with comparison data on macrofauna, *Deep Sea Res., Part I*, **45**, 625–638.
- Thistle, D., L. A. Levin, A. J. Gooday, O. Pfannkuche, and P. J. D. Lambshead (1999), Physical reworking by near-bottom flow alters the metazoan meiofauna of Fieberling Guyot (northeast Pacific), *Deep Sea Res., Part I*, **46**, 2041–2052.
- Thomas, D. J. (2004), Evidence for deep-water production in the North Pacific Ocean during the early Cenozoic warm interval, *Nature*, **430**, 65–68.
- Thomas, D. J., M. Lyle, T. C. Moore Jr., and D. K. Rea (2008), Paleogene deepwater mass composition of the tropical Pacific and implications for the thermohaline circulation in a greenhouse world, *Geochem. Geophys. Geosyst.*, **9**, Q02002, doi:10.1029/2007GC001748.
- Thomas, E. (1990), Late Cretaceous through Neogene deep-sea benthic foraminifera (Maud Rise, Weddell Sea, Antarctica), in *Proceedings of the Ocean Drilling Program Scientific Results*, vol. 113, edited by P. F. Barker et al., pp. 571–594, Ocean Drill. Program, College Station, Tex.
- Thomas, E. (1998), The biogeography of the late Paleocene benthic foraminiferal extinction, in *Late Paleocene-Early Eocene Biotic and Climatic Events in the Marine and Terrestrial Records*, edited by M. P. Aubry et al., pp. 214–243, Columbia Univ. Press, New York.
- Thomas, E. (2003), Extinction and food at the seafloor: A high-resolution benthic foraminiferal record across the initial Eocene thermal maximum, Southern Ocean Site 690, in *Causes and Consequences of Globally Warm Climates in the Early Paleogene*, Spec. Pap., vol. 369, edited by S. L. Wing et al., pp. 319–332, Geol. Soc. of Am., Boulder, Colo.
- Thomas, E. (2007), Cenozoic mass extinctions in the deep sea: What perturbs the largest habitat on Earth?, in *Large Ecosystem Perturbations: Causes and Consequences*, Spec. Pap., vol. 424, edited by S. Monechi et al., pp. 1–23, Geol. Soc. of Am., Boulder, Colo.
- Thomas, E., and N. J. Shackleton (1996), The Paleocene-Eocene benthic foraminiferal extinction and stable isotope anomalies, in *Correlation of the Early Paleogene in Northwest Europe*, Spec. Publ., vol. 101, edited by R. W. O'B. Know et al., pp. 401–441, Geol. Soc., London.
- Thomas, E., and J. C. Zachos (2000), Was the late Paleocene thermal maximum a unique event?, *Geol. Foeren. Stockholm Foerh.*, **122**, 169–170.
- Thomas, E., J. C. Zachos, and T. J. Bralower (2000), Deep-sea environments on a warm Earth: Latest Paleocene-early Eocene, in *Warm Climates in Earth History*, edited by B. Huber et al., pp. 132–160, Cambridge Univ. Press, Cambridge, U. K.
- Tjalsma, R. C., and G. P. Lohmann (1983), Paleocene-Eocene bathyal and abyssal benthic foraminifera from the Atlantic Ocean, *Micropaleontol. Spec. Publ.*, **4**, 1–89.
- Tripathi, A., and H. Elderfield (2005), Deep-sea temperature and circulation changes at the Paleocene-Eocene thermal maximum, *Science*, **308**, 1894–1898.
- van Morkhoven, F. P. C. M., W. A. Berggren, and A. S. Edwards (1986), *Cenozoic Cosmopolitan Deep-Water Benthic Foraminifera*, Bull. des Cent. de Rech. Explor.-Prod. Elf-Aquitaine, Mem., vol. 11, Elf Aquitaine, Pau, France.
- Webb, A. E., L. R. Leighton, S. A. Schellenberg, E. A. Landau, and E. Thomas (2009), Impact of Paleocene-Eocene global warming on microbenthic community structure: Using rank-abundance curves to quantify ecological response, *Geology*, **37**, 783–786.
- Westerhold, T., and U. Röhl (2013), Orbital pacing of Eocene climate during the Middle Eocene Climate Optimum and the chron C19r event: Missing link found in the tropical western Atlantic, *Geochem. Geophys. Geosyst.*, **14**, 4811–4825, doi:10.1002/ggge.20293.

- Wilson, C. D., and G. W. Boehlert (2004), Interaction of ocean currents and resident micronekton at a seamount in the central North Pacific, *J. Mar. Sci.*, *50*, 39–60.
- Winguth, A. M. E., E. Thomas, and C. Winguth (2012), Global decline in ocean ventilation, oxygenation, and productivity during the Paleocene-Eocene thermal maximum: Implications for the benthic extinction, *Geology*, *40*(3), 263–266.
- Yamaguchi, T., and R. D. Norris (2012), Deep-sea ostracode turnovers through the Paleocene-Eocene thermal maximum in DSDP Site 401, Bay of Biscay, North Atlantic, *Mar. Micropaleontol.*, *86–87*, 32–44.
- Yamaguchi, T., and R. D. Norris (2015), No place to retreat: Heavy extinction and delayed recovery on a Pacific guyot during the Paleocene-Eocene thermal maximum, *Geology*, *43*(5), 443–446.
- Yasuhara, M., G. Hunt, T. M. Cronin, N. Hokenishi, H. Kawahata, A. Tsujimoto, and M. Ishitake (2012), Climatic forcing of Quaternary deep-sea benthic communities in the North Pacific Ocean, *Paleobiology*, *38*, 162–179.
- Zachos, J., M. Pagani, L. Sloan, E. Thomas, and K. Billups (2001), Trends, rhythms, and aberrations in global climate 65 Ma to present, *Science*, *292*, 686–693.
- Zachos, J. C., M. W. Wara, S. Bohaty, M. L. Delaney, M. R. Petrizzo, A. Brill, T. J. Bralower, and I. Premoli-Silva (2003), A transient rise in tropical sea surface temperature during the Paleocene-Eocene thermal maximum, *Science*, *302*, 1551–1554.
- Zachos, J. C., et al. (2005), Rapid acidification of the ocean during the Paleocene-Eocene thermal maximum, *Science*, *308*, 1611–1615.
- Zachos, J. C., G. R. Dickens, and R. E. Zeebe (2008), An early Cenozoic perspective on greenhouse warming and carbon-cycle dynamics, *Nature*, *451*, 279–283.
- Zachos, J. C., H. McCarren, B. Murphy, U. Röhl, and T. Westerhold (2010), Tempo and scale of late Paleocene and early Eocene carbon isotope cycles: Implications for the origin of hyperthermals, *Earth Planet. Sci. Lett.*, *299*, 242–249.
- Zhou, X., E. Thomas, R. E. M. Rickaby, A. M. E. Winguth, and Z. Lu (2014), I/Ca evidence for global upper ocean deoxygenation during the Paleocene-Eocene thermal maximum (PETM), *Paleoceanography*, *29*, 964–975, doi:10.1002/2014PA002702.